1 **Phylogenomics of a genus of 'Great Speciators' reveals rampant incomplete lineage sorting,**
2 **gene flow, and mitochondrial capture in island systems**
3
4 Jenna M. McCullough[1,2*], Chad M. Eliason[3], Shannon Hackett[3], Corinne E. Myers[1], and Michael
5 J. Andersen[1]
6
7 *[1]Department of Biology and Museum of Southwestern Biology, University of New Mexico,*
8 *Albuquerque, NM, USA*
9 *[2]Department of Biology, University of Kentucky, Lexington, KY, USA*
10 *[3]Field Museum, Chicago, IL, USA*
11 **Corresponding author: Jenna McCullough[1], email jmmcculloughj@uky.edu*
12

ABSTRACT

The flora and fauna of island systems, especially those in the Indo-Pacific, are renowned for their high diversification rates and outsized contribution to the development of evolutionary theories. The total diversity of geographic radiations of many Indo-Pacific fauna is often incompletely sampled in phylogenetic studies due to the difficulty in obtaining single island endemic forms across the Pacific and the relatively poor performance of degraded DNA when using museum specimens for inference of evolutionary relationships. New methods for production and analysis of genome-wide datasets sourced from degraded DNA are facilitating insights into the complex evolutionary histories of these influential island faunas. Here, we leverage whole genome resequencing (20X average coverage) and extensive sampling of all taxonomic diversity within *Todiramphus* kingfishers, a rapid radiation of largely island endemic 'Great Speciators.' We find that whole genome datasets do not outright resolve the evolutionary relationships of this clade: four types of molecular markers (UCEs, BUSCOs, SNPs, and mtDNA) and tree building methods did not find a single well-supported and concordant species-level topology. We then uncover evidence of widespread incomplete lineage sorting and both ancient and contemporary gene flow and demonstrate how these factors contribute to conflicting evolutionary histories. Our complete taxonomic sampling allowed us to further identify a novel case of mitochondrial capture between two allopatric species, suggesting a potential historical (but since lost) hybrid zone as islands were successively colonized. Taken together, these results highlight how increased genomic and taxon sampling can reveal complex evolutionary patterns in rapid island radiations.

KEYWORDS: Artefactual branch effect, incomplete lineage sorting, Indo-Pacific, mitochondrial capture, incomplete, molecular phylogenetics, whole genome resequencing

Islands play an outsized role in the study of speciation of wild populations (Wallace 1881; MacArthur and Wilson 1967; Whittaker et al. 2017). Indeed, some of the most influential examples of species diversification stem from island systems. These include the adaptive radiations of Darwin's finches in the Galapagos (Darwin 1859; Grant and Grant 2006; Lamichhaney et al. 2015), Hawaiian silverswords and honeycreepers (Baldwin and Sanderson 1998; Lerner et al. 2011; Landis et al. 2018), and Caribbean *Anolis* lizards (Mahler et al. 2010). Though these examples have provided substantial insights in evolutionary biology, they are unique cases in which results may not be generalizable to other groups of organisms. Conversely, many lineages have evolved equally rapidly on islands without morphological novelty or obvious adaptive consequences—hereafter referred to as geographic radiations (Rundell and Price 2009; Simões et al. 2016). As distinct from adaptive radiations, geographic radiations occur across spatially structured landscapes, such as island archipelagos, without the evolution of key innovations or obvious adaptive changes (Moyle et al. 2009; Lieberman 2012; Moen and Morlon 2014). By studying organisms that occur across island systems, researchers can more readily parse how these forces shape the evolutionary history of clades during bouts of rapid and successive speciation events.

However, the study of rapid geographic radiations across island systems is not without its challenges. For example, neutral processes like genetic drift and mutation are stronger evolutionary forces in small populations such as those found in island systems (Baum et al. 2017). Additionally, rapid and successive speciation events contribute to short internode distances that prove difficult for phylogenetic inferences (Whitfield and Lockhart 2007; Bagley et al. 2020; Roycroft et al. 2020). These events also contribute to incomplete lineage sorting (ILS), which is more frequent when successive speciation events occur at a faster rate than the

coalescence of alleles (Degnan and Salter 2005; Maddison and Knowles 2006; Scornavacca and Galtier 2017). These issues are magnified when historical samples are included in analyses (Smith et al. 2020; Ernst et al. 2022; Roycroft et al. 2022), a necessary, yet adverse, byproduct of the gaps in modern genetic sampling. As our ability to collect better genetic data from degraded samples increases, empirical studies are turning to historical samples to include these range-restricted or rarely collected populations to broadly sample the entirety of geographic radiations.

The varied geographic radiations across the Indo-Pacific, encompassing southeast Asia eastward to Polynesia, have contributed to many aspects of ecological and evolutionary theories in wild populations. These include the early foundations of biogeography (Müller 1846; Wallace 1863, 1881; Lydekker 1896), the Theory of Island Biogeography (MacArthur & Wilson, 1967), the 'Great Speciator' paradox (Diamond et al., 1976), taxon cycles (Wilson, 1959, 1961), and allopatric speciation (Mayr 1942, 1963). Considered to be the main mechanism of speciation, allopatric speciation invokes geographic isolation as a critical aspect of reproductive isolation and subsequent lineage diversification. Prior to his work on speciation and the Biological Species concept (Dobzhansky 1937; BSC; Mayr 1940, 1942), Ernst Mayr wrote extensively on the phenotypic differences and evolutionary histories of many avian geographic radiations as curator of ornithology at the American Museum of Natural History. He was particularly interested in describing geographic variation based on avian specimens collected during the Whitney South Seas Expedition (Chapman 1935), including honeyeaters (Mayr 1932a), *Rhipidura* fantails (Mayr 1931a), *Pachycephala* whistlers (Mayr 1932b), and kingfishers (Mayr 1931b, 1935, 1941). The extensive phenotypic variation across these geographic radiations was influential in the development of his evolutionary theories (Mayr 1940, 1942, 1963). Mayr's work on the geographic variation of *Halcyon* kingfishers—now *Todiramphus* (Moyle 2006)—led to his

coinage of the 'superspecies' concept (Mayr 1931b), or what we now refer to as geographic radiations. The superspecies concept describes a taxonomic 'grey zone' in which the varied insular populations that comprise a geographic radiation may be recently diverged, having developed distinctive phenotypic characteristics in isolation; however, they could not be treated as separate species given our inability to assess reproductive isolation between allopatric populations, a requirement of the Biological Species concept (Dobzhansky 1937; Mayr 1942, 1963; Mayr and Diamond 2001).

Due to changing prevailing definitions of species and new advances in molecular systematics, there have been drastic impacts on the taxonomy of geographic radiations and subsequent estimations of their species richness. Alternative views on species boundaries, such as the Generalized Lineage Species Concept (de Quieroz 1998; de Queiroz 1999), led to an increase in recognized species-level diversity within allopatric superspecies complexes. For example, there has been a sea change in the way species limits are applied to insular geographic radiations, due to the resolution of paraphyly or recognition of phylogenetically divergent lineages, including in whistlers (Andersen et al. 2014; Marki et al. 2018), thrushes (Reeve et al. 2023), pittas (Irestedt et al. 2013), Australasian robins (Kearns et al. 2016), monarch flycatchers (Andersen et al. 2015a, 2021; McCullough et al. 2021), white-eyes (Lim et al. 2019), sunbirds (Ó Marcaigh et al. 2022), and kingfishers (Andersen et al. 2013; Sin et al. 2022). Increasingly, our understanding of speciation with gene flow in these radiations has brought a more nuanced approach to species limits (Nosil 2008; Campbell et al. 2018; Gyllenhaal et al. 2020; Mapel et al. 2021).

Todiramphus kingfishers represent the most species-rich and widespread genus within its taxonomic order (Aves: Coraciiformes), distributed from the Red Sea to French Polynesia (Fig.

1). They are generalist predators, not obligate plunge-diving piscivores, as their common name suggests. The Collared Kingfisher (*Todiramphus chloris*) is among the most widespread and polytypic avian superspecies complexes in the Indo-Pacific. Andersen et al. (2015b) argued for a revised classification based on a phylogeny that found no less than 10 species embedded within the *T. chloris* species complex, thus rendering *T. chloris* paraphyletic. Moreover, this study found that multiple instances of sympatry and obvious reproductive isolation within this group suggested that species limits within *Todiramphus*, and especially within the *T. chloris* species complex, were inadequately circumscribed.

Subsequent analyses highlighted the rapid diversification rate of *Todiramphus* kingfishers (Andersen et al. 2018; McCullough et al. 2019), rivaling the textbook geographic radiation of *Zosterops* white-eyes (Moyle et al. 2009; Lim et al. 2019). Unsurprisingly, the phylogenetic history of *Todiramphus* kingfishers has proven recalcitrant, likely owing to their high speciation rate and relative limitations of prior Sanger and reduced-representation sequencing datasets (Andersen et al. 2015b, 2018; McCullough et al. 2019). More focused work employing RADseq data, particularly assessing a major clade within the genus once considered a part of the *T. chloris* complex, has highlighted a case of mitochondrial discordance within one clade of *Todiramphus* comprising the migratory Sacred Kingfisher (*T. sanctus*), Islet Kingfisher (*T. colonus*), and Torresian Kingfisher (*T. sordidus*; DeRaad et al. 2023). However, this study found negligible levels of gene flow between these species and instead showed patterns consistent with high rates of incomplete lineage sorting.

Because of the relatively rapid timing and phylogenetic diversity in the group, *Todiramphus* kingfishers provide an opportunity to investigate how and when rapid radiations occur across the Indo-Pacific. *Todiramphus* kingfishers originated in Sahul (Australia and New

128 Guinea; Andersen et al. 2018), having diverged from its sister taxon *Syma* approximately 10.3
129 Ma (McCullough et al. 2019). Since then, they dispersed eastward to French Polynesia and
130 westward across Southeast Asia to western India and as far as the Arabian Peninsula (Fig. 1).
131 The genus exhibits a high degree of secondary sympatry in island systems. For example, five
132 *Todiramphus* species can be found on Halmahera Island, Indonesia (17,780 km^2; Woodall 2001),
133 and three species can be found on the much smaller Tetepare Island, Solomon Islands (118 km^2;
134 McCullough et al. 2023). These kingfishers show marked geographic diversity, with noticeable
135 differences in plumages and body size within the same archipelago (e.g., Cinnamon-banded
136 Kingfisher *T. australasia* in the Lesser Sundas) or continental landmasses (Blue-black Kingfisher
137 *T. nigrocyaneus* in New Guinea). Of the 29 currently recognized extant species of *Todiramphus*
138 (Clements et al.2023; Gill et al. 2024), 28 occur on islands and seven are single-island endemics
139 (Fry et al. 1992; Woodall 2001). At the subspecific level, for which there are 93 named taxa, 70
140 occur only on islands and 28 are restricted to single islands (Fig. S1). Indeed, they occur on
141 nearly every island from Southeast Asia, through Wallacea, Melanesia, Micronesia, and
142 Polynesia—they truly are a quintessential geographic radiation.

143 Various studies have addressed species-level relationships at the family and ordinal levels
144 (Moyle 2006; Andersen et al. 2018; McCullough et al. 2019) or have addressed specific clades
145 (Andersen et al. 2015b; O'Connell et al. 2019; DeRaad et al. 2023). Yet to date, only half of the
146 total taxonomic diversity within *Todiramphus* has been included in a phylogenetic analysis due
147 to the lack of accessible modern tissue samples. Owing to these sampling gaps, the taxonomy
148 and evolutionary history of *Todiramphus* kingfishers remains unresolved. In this study, we
149 employed whole-genome resequencing of all 93 extant *Todiramphus* taxa to produce the first
150 fully sampled phylogeny of one of Mayr's classic examples of a geographic radiation. From

whole genome resequencing data of 127 samples, we extracted four types of molecular data for phylogenetic inferences: ultraconserved elements (UCEs), single nucleotide polymorphisms (SNPs), Benchmarking Universal Single-Copy Orthologs (BUSCOs), and mitochondrial genomes (mtDNA). In doing so, we provide the most detailed study to date on the evolution of one of the most widespread of the 'Great Speciator' genera. Our results reveal how incomplete lineage sorting and gene flow during a rapid radiation have contributed to phylogenetic uncertainty as well as another case of mitochondrial discordance within this complex. Together, our study highlights the complicated evolutionary history of one of the Indo-pacific's greatest avian radiations.

METHODS

Sampling and laboratory methods

We sampled at least one individual for all extant and named *Todiramphus* taxa (Table S1). Because the number of taxa considered for each species varies widely, our species-level sampling ranged from a single sample representing the monotypic Somber Kingfisher (*T. funebris*) to 22 samples representing all the taxa within the widespread Pacific Kingfisher (*T. sacer*). We also sampled two populations of *T. sacer* that Mayr considered as possible separate taxa but refrained from naming both as separate subspecies, from Tucopia Island, Solomon Islands and Aneityum Island, Vanuatu (Mayr 1931b). Moreover, we sampled multiple individuals for two range-restricted Beach Kingfisher taxa that exhibit various head-color morphotypes (*T. saurophagus admiralitis* and *T. s. anachoreta* which have green/blue or white color on their heads). The only *Todiramphus* species we did not sample was the extinct Mangareva Kingfisher (*T. gambieri*), whose species is represented by a single specimen

174 collected from Mangareva Island in 1838 (Thibault and Cibois 2017). Many *Todiramphus* taxa
175 are endemic to a few or single islands across the Indo-Pacific and are thus rarely collected, so we
176 relied heavily on clippings of toepads from museum study skins (n = 76, 59% of total sampling).
177 All other samples were either sourced from blood (n = 4) or ethanol- or frozen-preserved tissue
178 samples (n = 47) loaned to us from natural history collections. Our sampling scheme spans
179 nearly one and a half centuries of collecting effort by countless collectors (1887–2019, toepads
180 span 1887–1987). In total, we had 127 samples representing all 92 extant diversity within the
181 genus; because of differing levels of sample quality, not all samples are present in each generated
182 dataset (Table S1). We chose four representatives from each of the three kingfisher subfamilies
183 as outgroups, sourced from higher-level work on genomic evolution across the family (Eliason et
184 al. 2023). Because DNA sourced from museum specimens is known to have higher rates of
185 degradation than high quality tissues, we treated toepad-sourced samples differently than tissue-
186 sourced samples at all stages of wet lab work (see Appendix 2 for more details). We prepared
187 libraries with Kapa Biosystems Hyper Prep Kit and the iTruStub dual-indexing system
188 (baddna.org) using established protocols at the University of New Mexico. We pooled toepad-
189 and tissue-sourced libraries separately (10–15 toepad libraries per lane and 15–16 tissue libraries
190 per lane) and sequenced them across 12 S4 PE-150 lanes of an Illumina NovaSeq 6000 at the
191 Oklahoma Medical Research Foundation.
192
193 *Bioinformatic processing*
194 We trimmed demultiplexed raw reads with trimmomatic v.0.39 (Bolger et al. 2014) and aligned
195 cleaned reads to a Collared Kingfisher (*T. chloris collaris*) reference genome (Eliason et al.
196 2022) using BWA v.0.7.17 (Li and Durbin 2009) and GNU Parallel (Tange 2021). We used

197 MarkDuplicatesSpark, implemented in GATK v.4.2.6.1 (McKenna et al. 2010; Van der Auwera
198 and O'Connor 2020), to tag and remove duplicate reads. We assessed individual genome
199 summary statistics (i.e., CollectAlignmentSummaryMetrics, CollectInsertSizeMetrics, and
200 depth) with Picard v.2.26.11 (Broad Institute 2019) and samtools v.1.15 (Danecek et al. 2021).
201 We used GATK v.3.8.1 to identify and realign indels (RealignerTargetCreator, IndelRealigner)
202 to produce final BAM files for extraction of different types of molecular markers for downstream
203 phylogenetic analyses.
204
205 *Extraction and analysis of Ultraconserved Elements (UCEs)*
206 We used the Phyluce v.1.7.0 (Faircloth 2016); described in full at https://github.com/faircloth-
207 lab/ phyluce) Python package to harvest thousands of UCE loci in silico (specifically following
208 the phyluce Tutorial III: Harvesting UCE Loci From genomes). We used samtools to convert the
209 final BAM file to fasta and then to 2.bit format using fatoTwoBit (Kuhn et al. 2013). Next, we
210 aligned the tetrapods UCE 5k probe set to each genome and extracted loci with 500 bp flanking
211 regions with "phyluce_probe_slice _sequence_from_genomes". We then followed the typical
212 bioinformatic steps implemented in the phyluce pipeline starting from "phyluce_assembly_get
213 _match_counts." We aligned each locus with MAFFT (Katoh and Standley 2013) without
214 initially trimming the ends of UCE loci, instead trimming using TrimAL v.1.4.rev15 (Capella-
215 Gutiérrez et al. 2009) with the "-automated1" flag and degenerated_DNA matrix (available at
216 https://github.com/inab/trimal/ blob/trimAl/dataset/matrix.Degenerated_DNA) to allow for
217 ambiguous bases.
218 During preliminary phylogenetic exploration, we determined that many of the toepad-
219 sourced samples had exceptionally long branches (see below for phylogenetic analyses and Table

220 S1 for these samples). Biologically unrealistic long branches such as these can contribute to
221 long-branch attraction and therefore incorrect phylogenetic relationships (Felsenstein 1978); this
222 issue has been shown as a byproduct of poor alignment trimming contributing to "dirty ends" of
223 UCE loci sourced from historical samples, including those sourced from avian toepads
224 (McCormack et al. 2015; Smith et al. 2020; Salter et al. 2022). We removed these artefactual
225 "dirty ends" following the bioinformatic pipeline by Smith et al. (2020; see Appendix 2 for
226 further information). Our final UCE dataset was a 90% complete matrix comprising multiple
227 individuals for some taxa that had at least 105 of 117 samples present at each UCE locus (Table
228 S3).

229 We used multispecies coalescent tree (MSC) and concatenated maximum likelihood
230 (ML) methods to analyze UCE datasets. Because gene tree histories could conflict with the
231 overall species tree, we used two species tree methods that account for gene tree heterogeneity
232 (Kubatko and Knowles 2023). First, we used SVDquartets (Chifman and Kubatko 2014)
233 implemented in Paup* 4.0a168 (Swofford 2003); this quartet-based method uses a concatenated
234 alignment and site pattern frequencies of splits to estimate a species tree and has been shown to
235 perform well for large multilocus datasets (Wascher and Kubatko 2021). To decrease
236 computation time in Paup*, we split up the 117-sample, 90% complete matrix into two,
237 overlapping subsets of taxa (each with 69 samples). For each subset, we analyzed all possible
238 quartets and assessed support with 100 BS. Next, we used the summary-statistic method
239 ASTRAL-III v.1.15.2.4 (Zhang et al. 2018; Rabiee et al. 2019) to estimate the species tree. This
240 summary-statistic MSC method is sensitive to fragmentary data and depends on high quality
241 gene trees (Mirarab 2023). Because toepad-sourced samples often have a higher degree of
242 missing data within individual alignments, we used a series of filtering steps to produce a final

243 set of high quality gene trees. To do so, we 1) filtered the 90% complete matrix to drop samples
244 from individual alignments if they comprised more than 25% of ambiguous nucleotides (N) and
245 70% of gaps; 2) filtered our gene trees based on different thresholds of parsimony informative
246 (PI) sites (>50 PI sites and 1,583 gene trees; >100 PI sites and 125 gene trees; see Appendix 2
247 for more details). For ASTRAL, we increased the number of searches (-r) and subsampling (-s)
248 from the default of 4 to 8. To estimate a concatenated ML phylogeny of the 90% complete
249 matrix, we used RaxML-NG v.1.2.0 (Kozlov et al. 2019), assuming a general time-reversible
250 model of nucleotide substitution and gamma-distributed rates among all sites (GTR+G) and
251 evaluated support with the autoMRE function (set to 1000 BS). Finally, we inferred a partitioned
252 maximum likelihood phylogeny with IQtree 2.1.4 (Chernomor et al. 2016; Minh et al. 2020b),
253 implementing modelfinder and assessing support with 1,000 replicates of Ultrafast bootstraps
254 (Hoang et al. 2018).
255
256 *Processing and analysis of single-copy orthologous loci (BUSCOs)*
257 Because of their conserved nature in coding regions of the genome, single-copy orthologous
258 genes (Benchmarking Universal Single-Copy Orthologs [BUSCOs; Simão et al. 2015) have been
259 shown to be informative molecular markers at both deep and shallow timescales (Waterhouse et
260 al. 2018; Timilsena et al. 2022; Alaei Kakhki et al. 2023). Prior to extracting thousands of
261 BUSCO loci for phylogenetic inference, we masked low coverage sites from the final BAM files.
262 Generally, we calculated read depths with mosdepth 0.3.3 (Pedersen and Quinlan 2017),
263 generated consensus sequences with bcftools 1.19 (Li 2011; Danecek and McCarthy 2017)
264 implemented in a custom function in R 4.3.2 (R Development Core Team 2013), and used
265 bedtools v2.31.1 (Quinlan and Hall 2010) to mask sites with less than five reads. We extracted

266 thousands of BUSCO loci from the genomes using BUSCO 5.4.6 (Manni et al. 2021a, 2021b).
267 During initial phylogenomic analysis, it became clear that extracting these data from the lower
268 coverage toepad genomes yielded problematic alignments that contributed to an artificial pattern
269 in which these low coverage toepad genomes grouped together rather than within the clades that
270 matched those inferred with SNP and UCE datastets (Fig. S3). Because all of these data are
271 aligned to the same reference, we instead ran BUSCO on the high quality *T. chloris collaris*
272 reference genome and used BED coordinates of 8,337 BUSCO loci to extract these same regions
273 from all of our samples. To do so, we converted the metaeuk output for our reference sample to
274 gff3 coordinate format using the python script MetaeukToGff.py (https://github.com/Andy- B-
275 123/MetaeukToGff3). With GFFread v0.12.8 (Pertea and Pertea 2020), we extracted individual
276 genes in amino acid (AA) format from all samples. We created locus-specific files with
277 faSomeRecords (Kuhn et al. 2013) and removed short duplicates within loci with keep-
278 longest.py (https://gist.github.com/mkweskin/8869358). Because all loci—regardless of whether
279 adequate coverage of sequence data is present—are extracted based on this approach, we filtered
280 out loci that were entirely composed of missing data or invariant sites as well as those that did
281 not have PI sites to produce a matrix of 8,012 AA loci for 109 samples.
282 To determine if protein-coding loci inferred similar phylogenetic histories to the SNP and
283 UCE datasets, we also inferred phylogenies for the BUSCO loci with MSC and ML methods.
284 Similar to how we treated UCE data, we performed additional steps to filter BUSCO loci for
285 MSC analyses in order to produce high quality gene trees as input into ASTRAL. Though every
286 sample in our dataset was present at each of these loci regardless of presence of data, many
287 toepad samples comprised 50% or more of ambiguous sites. We dropped these individual
288 samples from BUSCO alignments with the same python script noted in the UCE processing

289 section by the ambiguous character from “N” to “X”. In a similar fashion as the UCE datasets,
290 we filtered BUSCO loci by the number of PI sites. With a threshold of 20 PI AA sites (4,177
291 gene trees), a similar artefactual pattern of toepad-sourced samples cluster was apparent (Fig. S4)
292 that disappeared with a threshold of 100 PI AA sites (470 gene trees). We increased the number
293 of searches (-r) and subsampling (-s) to 8. We inferred a maximum likelihood phylogeny for the
294 concatenated matrix of 8,012 loci with IQtree 2.1.4 and assessed support with 1,000 ultrafast
295 bootstraps. During model selection, we confined substitution models to the Q.bird matrix and did
296 not allow for partition merging (Chernomor et al. 2016; Kalyaanamoorthy et al. 2017; Minh et al.
297 2021).
298
299 *Processing and analysis of Single Nucleotide Polymorphisms (SNPs)*
300 We performed variant discovery and genotyping on realigned BAM files with UnifiedGenotyper
301 in GATK 3 using a scatter-gather approach. Recent work has shown that the results of this
302 program are comparable to HaplotypeCaller in GATK 4 and ANGSD (Korneliussen et al. 2014)
303 for non-model organisms (Aguillon et al. 2021). With VCFtools, we initially filtered SNPs that
304 were successfully genotyped in at least 90% of samples, had a minimum quality score of 30,
305 minimum depth of 3, and a minor allele count of 3. Because toepad-sourced samples had
306 significantly higher missing data, we removed samples that were missing at 55% or more sites in
307 this initial dataset. This only affected poorly sequenced toepad-sourced samples in which we had
308 several representatives per taxon. One sample of *T. n. nigrocyaneus* (AMNH 301866) fell
309 marginally below this threshold, but since it had less missing data than our other *T. n.*
310 *nigrocyaneus* sample, thus we still included it in the final VCF file (see Table S1). After
311 dropping these six toepad samples, we then produced a SNP dataset in which all samples were

312 successfully genotyped at all sites, as well as only keeping bi-allelic SNPs every 5,000 bp. Our
313 final dataset comprised 85,156 SNPs from 119 samples representing all *Todiramphus* taxa.
314 We implemented three different ML, MSC, and distance-based network methods for tree
315 building using SNP data. First, we converted the VCF file to nexus format with nucleotide data
316 using the ruby script convert_vcf_to_nexus.rb (available on https://github.com/mmatschiner/
317 tutorials/blob/master/species_tree_inference_with_snp_data/src/convert_vcf_to_nexus.rb). We
318 used this alignment for ML inference in IQtree, correcting for ascertainment bias (+ASC) to limit
319 branch length overestimations and assessed support with 1,000 BS replicates. Second, we
320 analyzed the SNP alignment using all possible quartets with SVQquartets and assessed support
321 with 1,000 BS replicates. Third, we generated a phylogenetic network to visualize the genetic
322 distances between all samples. We used R package StAMPP v1.6.3 (Pembleton et al. 2013; R
323 Development Core Team 2013) to produce a pairwise genetic distance (Nei's D; Nei 1972)
324 matrix as input into SplitsTree4 v 4.18.13 (Bryant and Moulton 2004; Huson and Bryant 2006)
325 to produce a Neighbor-Net phylogram.
326
327 *Extraction and analysis of Mitochondrial genomes*
328 We generated mitogenomes by mapping the trimmomatic cleaned reads to a reference
329 mitogenome of *T. sanctus vagans* (GenBank: NC011712, (Pratt et al. 2009) using the singularity
330 version of Mitofinder V1.4.1 (Allio et al. 2020). We checked these alignments by eye for
331 incorrect internal stop codons and dropped spurious samples from gene alignments if initial
332 phylogenetic analyses inferred them as an outgroup to *Todiramphus* (suggesting a incorrectly
333 mapped NUMT sequence rather than true mitochondrial DNA; (Nacer and Raposo do Amaral

334 2017). We used IQtree v2.2.2.6 to infer a maximum likelihood phylogeny of the 12 mtDNA
335 genes and assessed support with 1,000 BS replicates.
336
337 *Tests for incomplete lineage sorting and gene flow*
338 To test for incomplete lineage sorting, we calculated gene and site concordance factors
339 for the BUSCO and 90% complete UCE matrix trees inferred with IQtree. Gene (gCFs) and site
340 concordance factors (sCFs) are two additional measures for assessing topological support by
341 revealing the level of gene tree species tree discordance in phylogenomic datasets to assess the
342 extent of ILS. We pared down each of these datasets to a subset of 34 tips that encompassed
343 higher-level relationships across *Todiramphus*. To calculate gCFs, we chose to use the more
344 informative gene trees that we produced for ASTRAL in order to limit noise introduced by
345 thousands of low-signal gene trees. We calculated cGFs from UCE-based gene trees with >50
346 PIsites (1,583 gene trees) and BUSCO-based gene trees with >20 PI AA sites (4,155 gene trees)
347 with the superfluous tips not included in our 34-tip subset dropped ad hoc. We calculated sCFs,
348 using the maximum likelihood implementation with --scfl flag (Minh et al. 2020a; Mo et al.
349 2023), from the pared down concatenated alignments.
350 We estimated the phylogenetic network for the UCE gene tree dataset (1,583 gene trees)
351 with Species Networks applying Quartets (SNaQ; Solís-Lemus and Ané 2016) implemented in
352 Julia (Bezanson et al. 2017). SNaQ is a maximum pseudolikelihood approach to infer
353 phylogenetic networks while simultaneously accounting for ILS and gene flow with a coalescent
354 model based on quartet concordance factors (Baum 2007). We counted quartets and calculated
355 concordance factors with the 'countquartetsintrees' function in PhyloNetworks (Solís-Lemus et
356 al. 2017). After removing our outgroup, the Blue-caped Kingfisher (*Actenoides hombroni*), from

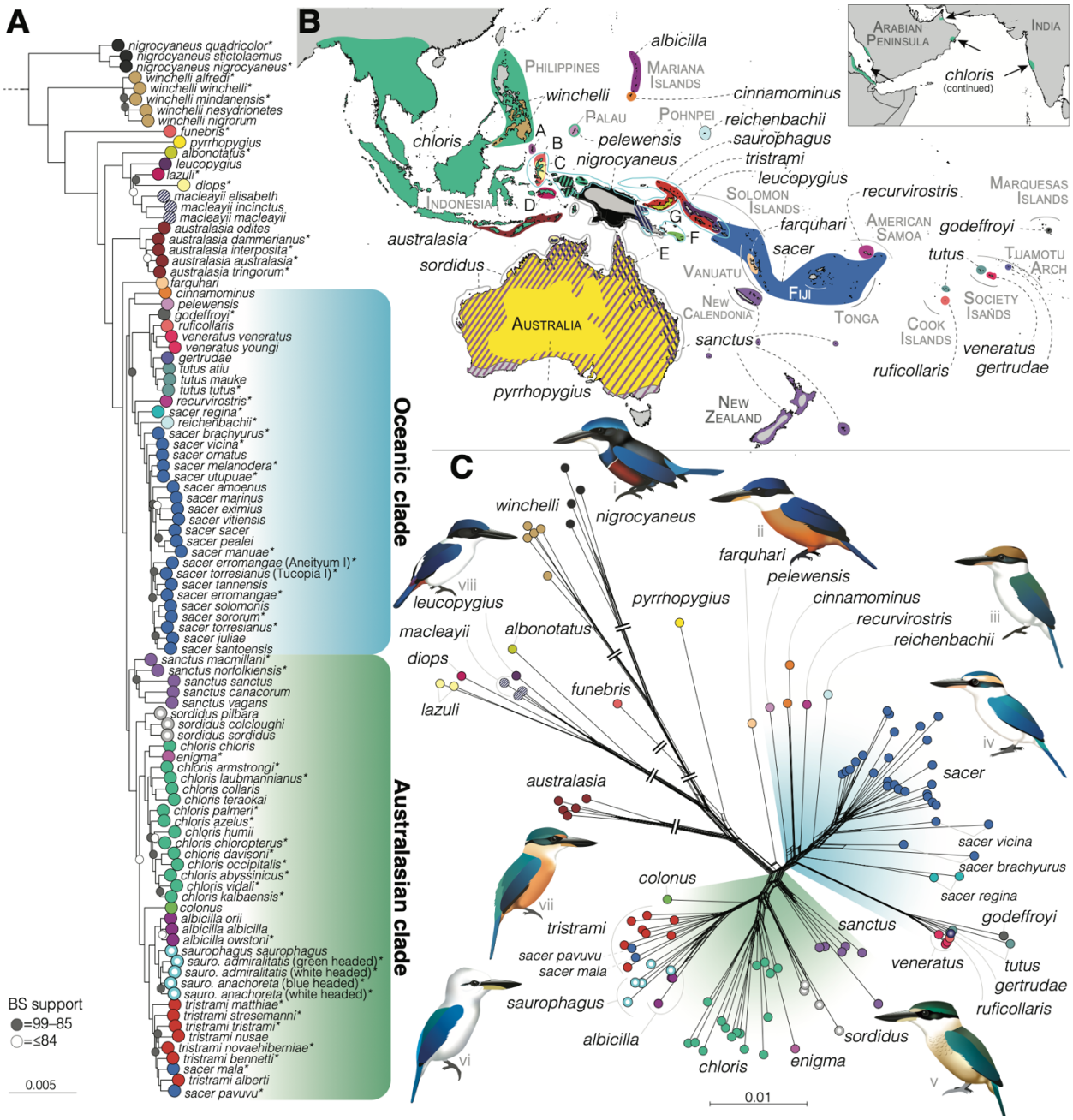

357

358 **Figure 1.** Ranges and evolutionary relationships of all *Todiramphus* kingfishers. A) Partitioned
359 maximum likelihood phylogeny of 4,942 UCE loci from the 90% complete matrix. Circles on nodes
360 indicate support values less than 100 bootstrap support. B). Ranges of 29 species-level groups with
361 diagonal lines showing sympatry and colors corresponding to tips. Letters corresponding to species
362 ranges are as follows: A, *T. enigma;* B, *T. funebris;* C, *T. diops;* D, *T. lazuli*; E, *T. macleayii*, F, *T.*
363 *colonus*, G, *T. albonotatus*. See Figure S1 with these ranges directly labeled with taxon names. C)

Unrooted phylogenetic network based on pairwise divergence among all samples, produced from a complete set of 85,165 SNPs. Note that some branch lengths have been artificially shortened, denoted by double slashes. See Figure S17 for subspecific labels. Illustrations created by Jenna McCullough and names are as follows: i, *T. nigrocyaneus*; ii, *T. farquhari*; iii, *T. reichenbachii;* iv, *T. sacer*; v, *T. sanctus*; vi, *T. saurophagus*; vii, *T. tristrami*; and viii, *T. leucopygius.*

our gene trees, our 33-tip dataset comprised 40,920 unique quartets which proved computationally intractable to analyze together. Instead, we produced three subsets of 3,000 non-overlapping randomly selected quartets as input into SNaQ, using h_m= 0–4 with 10 runs each. For each subset, we kept adding edges until the likelihood scores no longer improved and chose the tree with the best overall likelihood (though we report the best tree for each subset).

Mitochondrial data revealed discordant topologies for some *T. sacer* taxa and *T. colonus* and *T. sordidus* (discussed in detail in the Results section); to specifically test for gene flow between non-sister taxa, we used Dsuite v0.5 (Malinsky et al. 2021) to perform four-taxon ABBA-BABA tests. We used our 119-sample filtered SNP dataset, in which each sample was present at a given site and each SNP was at least 5,000 bp apart (85,156 SNPs) as input and used the *Dtrios* module for block Jackknifing of 20 SNP windows across the genome (4,256 SNPs per window) to calculate D and f_4-ratio statistics (Durand et al. 2011; Patterson et al. 2012) for every possible quartet topology. We analyzed two different datasets: 1) a species-level dataset in which all subspecific taxa were lumped into their respective species' tip, except for *T. sacer regina* (as it was not monophyletic with the rest of *T. sacer*; see Results) and 2) the same as #1 but pared down for fewer species and the treatment of five *T. sacer* taxa that were recovered within the mitochondrial *T. sanctus* clade as separate tips: *T. sacer vicina* and four microendemics of Temotu Province, Solomon Islands, *T s. regina, vicina, ornatus, utupuae,* and *brachyurus*. The

388 remaining *T. sacer* taxa were grouped within a "polynesian" and "melanesian" tip based on the
389 two clades recovered in the UCE IQtree topology (Fig. 1). We incorporated a false discovery rate
390 (FDR)-adjusted statistical significance threshold (Benjamini and Hochberg 1995), which is
391 recommended by the developer when running more than one trio (Malinsky et al. 2021). Our
392 FDR-adjusted *p*-threshold was 0.0000137 (3,654 pairwise tests for 29 tips in both datasets).
393

394 RESULTS

395 The average coverage of assembled genomes was 20X with differences between toepad- (n = 66,
396 average depth 10X with range of 4.6–27.9X) and tissue-sourced genomes (n = 47, average depth
397 34.8X, 11.9–98X; Table S1, Fig S5). Tissue-sourced genomes were relatively complete, with an
398 average 96.2% (standard deviation ±0.72%) of the 8,338 single-copy BUSCO loci (Table S4,
399 Figs. S6–7). Toepad-sourced genomes, on the other hand, averaged 55.9 ± 33.7% single-copy
400 BUSCO loci; though this was higher for those with more than 10X average coverage (88 ±
401 14.9%). Average depth for toepad-sourced genomes did not negatively scale with collection date;
402 perhaps not surprisingly, the relative data quality from the datasets extracted from these genomes
403 did scale with average depth (Fig. S7). Ten of the 127 genomes produced for this project, all
404 sourced from toepad material, were not high enough in coverage to produce adequate data for
405 inclusion in each of the four genetic datasets (we highlight in which datasets samples were
406 present in Table S1).

407 We extracted several datasets with varying numbers of samples for UCE, BUSCO, SNP,
408 and mtDNA data (Table S3). Our 90% complete UCE matrix with 117 samples comprised 4,942
409 loci and 4,531,264 bp. Our BUSCO datasets, differing based on thresholds of within-locus PI
410 AA sites, comprised 8,012 (>20 PI sites per locus threshold, total length 5,102,241 AA sites)

with 108 samples. Our 100% complete SNP dataset, with one SNP per 5 kb, comprised 85,156 SNPs for 119 samples. We recovered complete or partial mitochondrial genomes for 111 samples.

Topological conflict between nuclear data types and tree-building methods

The backbone of the *Todiramphus* tree is characterized by many short internodes, suggesting rapid and successive speciation events early in the evolution of this group. We found phylogenetic conflict between datasets and methods due, in part, to these short internodes. When just considering species-level relationships, we did not find a single well-resolved topology that matched across any two datasets or tree-building methods (Fig. 2). The first three main branches of the tree rarely varied across analyses, with Blue-black Kingfisher (*T. nigrocyaneus*), Rufous-lored Kingfisher (*T. winchelli*), and Sombre Kingfisher (*T. funebris*), respectively. Only in one analysis did we find *T. winchelli* fully supported as the first branch of the genus instead of *T. nigrocyaneus* (UCE SVDquartets tree; Fig. S8). We found conflicting phylogenetic signals for the next major branch (Fig. 2), as we either recovered: 1) the Australian endemic Rufous-backed Kingfisher (*T. pyrrhopygius*; Figs. S9–10), 2) a small clade of four species as the next branch (referred to as the "*leucopygius* clade"; Figs. 1, S11–18), or 3) *T. pyrrhopygius* sister to the *leucopygius* clade (Fig. S8). Gene and site concordance factors for the UCE and BUSCO IQtree-inferred topologies revealed that both datatypes strongly favored conflicting topologies: 76% of 1,583 best UCE gene trees and 59% of concatenated 90% complete UCE alignment (4,531,264 bp in length) favored the earlier branching *T. pyrrhopygius* topology whereas a similar percentage of the significantly larger BUSCO dataset (4,155 gene trees and 5,102,241 AA sites) favored the *leucopygius* clade branching prior to *T. pyrrhopygius* (Fig. 3). The Lesser Sundas

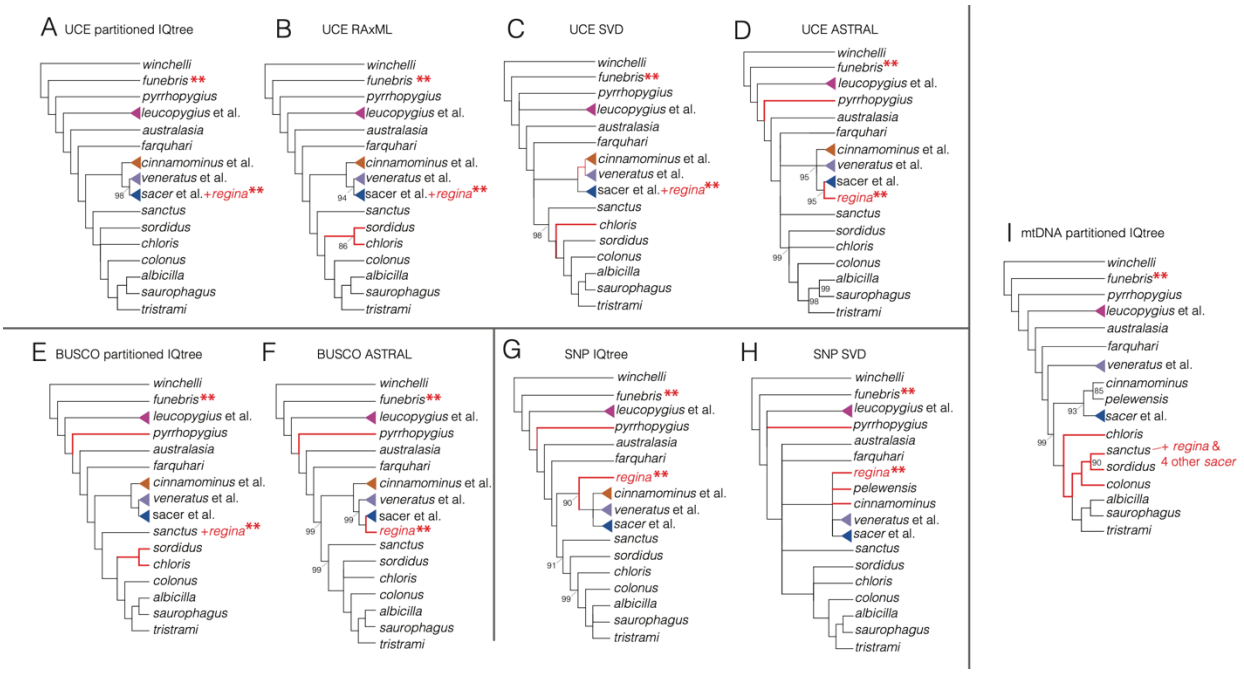

Figure 2. Comparisons of trees from UCE, BUSCO, SNP, and mtDNA datasets with red branches highlighting differences from the UCE maximum likelihood tree. Double asterisks (**) indicate samples sourced from toepad samples. We collapsed nodes with <85 bootstrap support and note those with 99–85 BS. We grouped lineages that were consistently inferred as a clade for simplicity: *T. sacer* et al. includes *T. reichenbachii* and *T. recurvirositris*. Note that *T. pelewensis* and *T. cinnamominus* are considered a single tip ("*cinnamominus* et al..") except in Panels H and I.

endemic species, Cinnamon-banded Kingfisher (*T. australasia*) was always supported as sister to the clade comprising the bulk of diversity within the genus: the Vanuatu Kingfisher (*T. farquhari*) and all other species. We consistently found support for two major clades within *Todiramphus*: 1) an entirely oceanic island clade and 2) an Australasian clade (Fig. 1). We hereafter refer to these as the "Oceanic clade" and the "Australasian clade" even though some taxa within the Australasian clade also inhabit oceanic islands.

Within the Oceanic clade, we found support for three subclades: 1) a subclade of two microendemics in Micronesia, the Palau Kingfisher (*T. pelewensis*) and the extinct-in-the-wild Guam Kingfisher (*T. cinnamominus*), 2) a subclade of eastern Polynesian species (referred to hereafter as such, comprising *T. veneratus*, *T. gertrudae, T. tutus* etc.), and 3) a subclade comprising Flat-billed Kingfisher (*T. recurvirostris*), Pohnpei Kingfisher (*T. reichenbachii*), and *T. sacer* (i.e., the "*sacer* clade") sister to the Polynesian subclade. The relationships between these subclades were largely consistent, even though sCF of the relationship between the east Polynesian clade and the *sacer* clade showed that alternative topologies were favored at nearly the same proportion as the inferred topologies for both BUSCO and UCE datasets (Fig. 3). However, most of the discordance between analyses and data types were mostly restricted to whether *T. recurvirostris* and *T. sacer regina* diverged earlier than *T. reichenbachii* and crown *T. sacer* (supported by UCE data; Figs. S8–11, 15) or not (supported by SNP and BUSCO data; Figs. S13–14, 16). Whereas the placement of *T. sacer regina* (Wallis and Futuna), represented by two toepad-sourced genomes (6.8 and 14.5 average coverage), varied between different clades across analyses, we never inferred a topology in which *T. sacer regina* was within crown *T. sacer*. UCE ML analyses instead found *T. s. regina* sandwiched between two other microendemic species in a ladderized branching pattern: *T. recurvirostris* (Samoa), *T. s. regina*, and *T. reichenbachii* (Pohnpei I.; Figs. S1, S9–10). With some support, we also found *T. s. regina*: 1) sister to *T. recurvirostris* (Fig. S8), 2) branching prior to *T. recurvirostris* (Fig. S15), 3) as the first branch of the Oceanic clade (Fig. S14), or 4) as the first branch within the *T. sanctus* complex (Fig. S16). The unrooted phylogenetic network placed *T. sacer regina* as similarly distant from *T. sacer* as *T. recurvirostris* (Figs. 1C; S17).

Within the Australasian clade, eight species formed four subclades: three species complexes (Sacred Kingfisher *T. sanctus,* Torresian Kingfisher *T. sordidus*, and Collared Kingfisher *T. chloris*) and a clade comprising the largely oceanic island species (Islet Kingfisher *T. colonus*, Mariana Kingfisher *T. albicilla*, Beach Kingfisher *T. saurophagus*, and Melanesian Kingfisher *T. tristrami*). *Todiramphus sanctus*, one the few migratory species in the genus (though four of five subspecies are sedentary and endemic to Pacific Islands), was supported as the first branch in the Australasian clade. Across the nuclear datasets, most of the species-level discordance between analyses centered on the second branch within the clade: whether it was *T. sordidus* (Figs. S8B, 14)*, T. chloris* (Fig. S8A)*,* a sister relationship between the two (Figs. S10, 16), or so poorly supported we considered it a polytomy with the *colonus* clade (Figs. S9, 11–13, 15).

Mitochondrial discordance and new cases of mtDNA capture within Todiramphus

Compared to nuclear DNA, the mitochondrial data revealed a different picture of the evolutionary history of *Todiramphus* kingfishers in three major ways (Figs. 4, S19). First, the mtDNA-inferred topology matched the ML UCE data in which *pyrrhopygius* diverges prior to the *"leucopygius"* clade (Figs. S9–10, 18). Second, it was the only dataset to show the eastern Polynesian clade (i.e., *T. veneratus* et al.) sister to the rest of the Oceanic clade and Australasian clade. Third, it was the only phylogeny to recover *T. chloris* as the first branch of the Australasian clade and instead recover a significantly different topology from all nuclear datasets: *T. colonus* sister to *T. sanctus* and *T. sordidus*. This relationship has been highlighted before (DeRaad et al. 2023) and was therefore expected. However, we recovered a strongly supported topology of five *T. sacer* taxa embedded within the *T. sanctus* clade, most

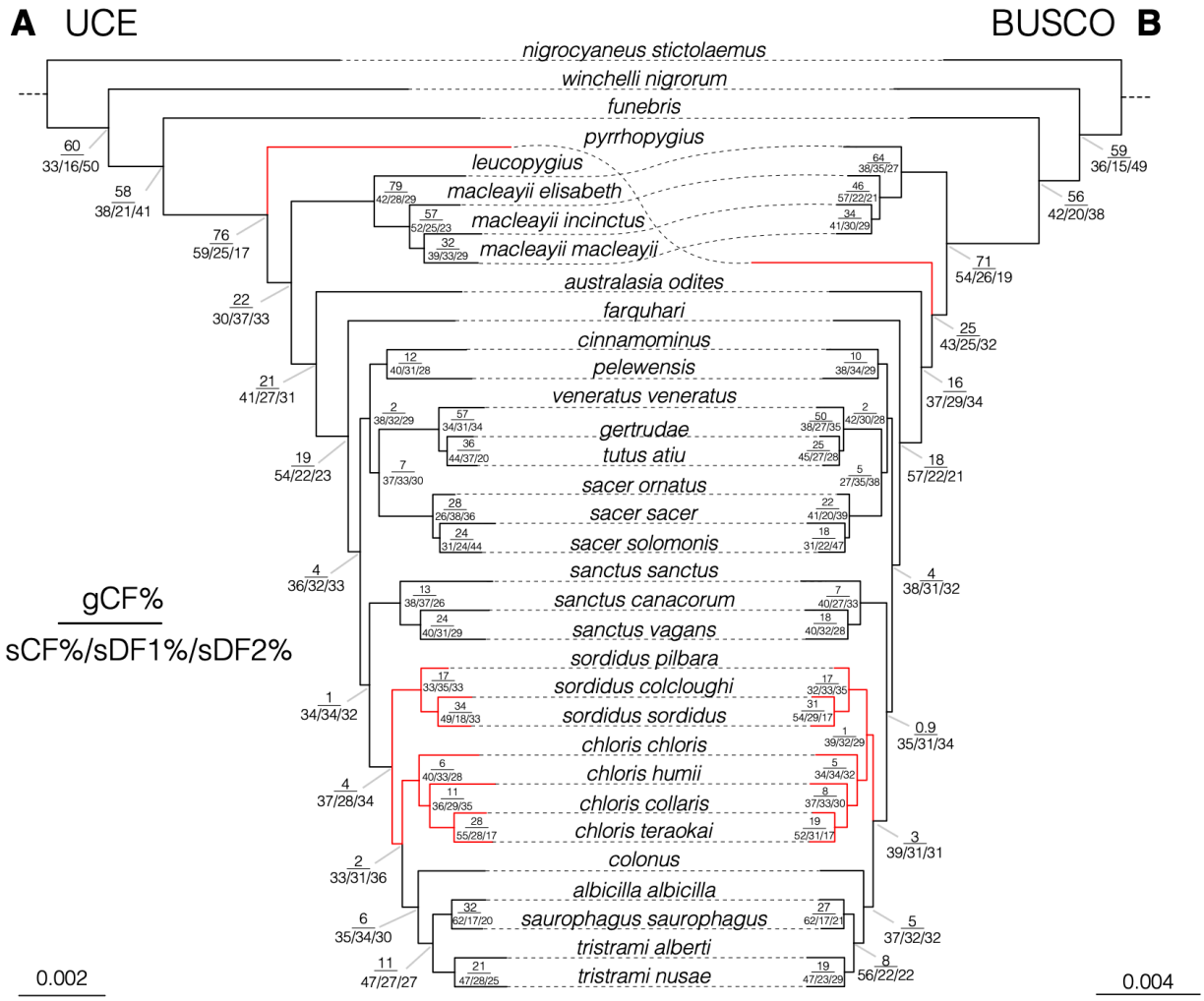

Figure 3. Site (sCF) and gene (gCF) concordance factors of UCE and BUSCO topologies show a high degree of ILS present in the evolutionary history of *Todiramphus* kingfishers. A) Partitioned 90% complete UCE matrix (4,942 loci, total 4,531,264 bp) inferred in IQtree with gCFs calculated from gene trees of loci with at least 50 parsimony informative sites (PIs; 1,583 gene trees). B) Partitioned BUSCO topology (8,012 loci, total 5,102,241 amino acid sites) inferred in IQtree with gCFs calculated from gene trees of loci with >50 PI amino acid sites (4,155 gene trees).

closely associated with the migratory taxon *T. s. sanctus* and sedentary *T. sanctus macmillani* (endemic to Loyalty Islands, NE of New Caledonia). This group of *T. sacer* taxa with *T. sanctus*

503 mitochondrial DNA included *T. sacer regina* and four allopatric microendemics of Temotu
504 Province of Solomon Islands (*T. sacer ornatus, vicina, brachyurus,* and *utupuae*). Apart from our
505 inability to determine the relationship of *T. s. regina* with nuclear data, these four other Temotu
506 *T. sacer* taxa were either supported as the first few sequentially branching lineages of the *T.*
507 *sacer* clade (Figs. S9–10, 14–16) or had equivocal support values deeper in the *sacer* complex
508 (Figs. S11, 14–15) across nuclear datasets. In the unrooted phylogenetic network, three of these
509 five taxa were inferred to be early branching and independent lineages on par with splits shown
510 in other species-level taxa (i.e., *T. recurvirostris* and *T. reichenbachii*; Figs. 1C, S17). We had
511 sequenced multiple individuals of all these taxa (n = 2–3 samples) to confirm their curious
512 placement as sequentially branching at the base of the *T. sacer* complex. Yet, we did not find that
513 all individuals of each taxon had *T. sanctus* mtDNA: *T. sacer ornatus* and *T. sacer vicina* had at
514 least one individual in *T. sanctus* and *T. sacer* clades, whereas all samples for *T. sacer*
515 *brachyurus, regina,* and *utupuae* were recovered within *T. sanctus*.
516
517 *Patterns of gene flow*
518 ABBA-BABA tests uncovered biologically plausible scenarios of gene flow across both subsets
519 of data (species-level and the pared down dataset to investigate gene flow between *T. sanctus*
520 and *T. sacer* taxa that have *T. sanctus* mtDNA). Of the 3,544 calculated D-statistics, 858 and
521 887, respectively, were significant with a FDR-adjusted p value <0.000013. The results show
522 complex patterns highlighting gene flow between *T. sanctus* and mitochondrial discordant
523 lineages, with elevated F4 ratios between *T. sanctus* and *T. colonus* (F4 = 0.34), *T. sordidus* (F4
524 = 0.31), *T. s. regina* (F4 = 0.34), and the four Temotu *T. sacer* taxa (range of F4 = 0.12–0.33;
525 Figs. S19–20). Though the highest F4 ratios in the pared down dataset are between *T. sacer*

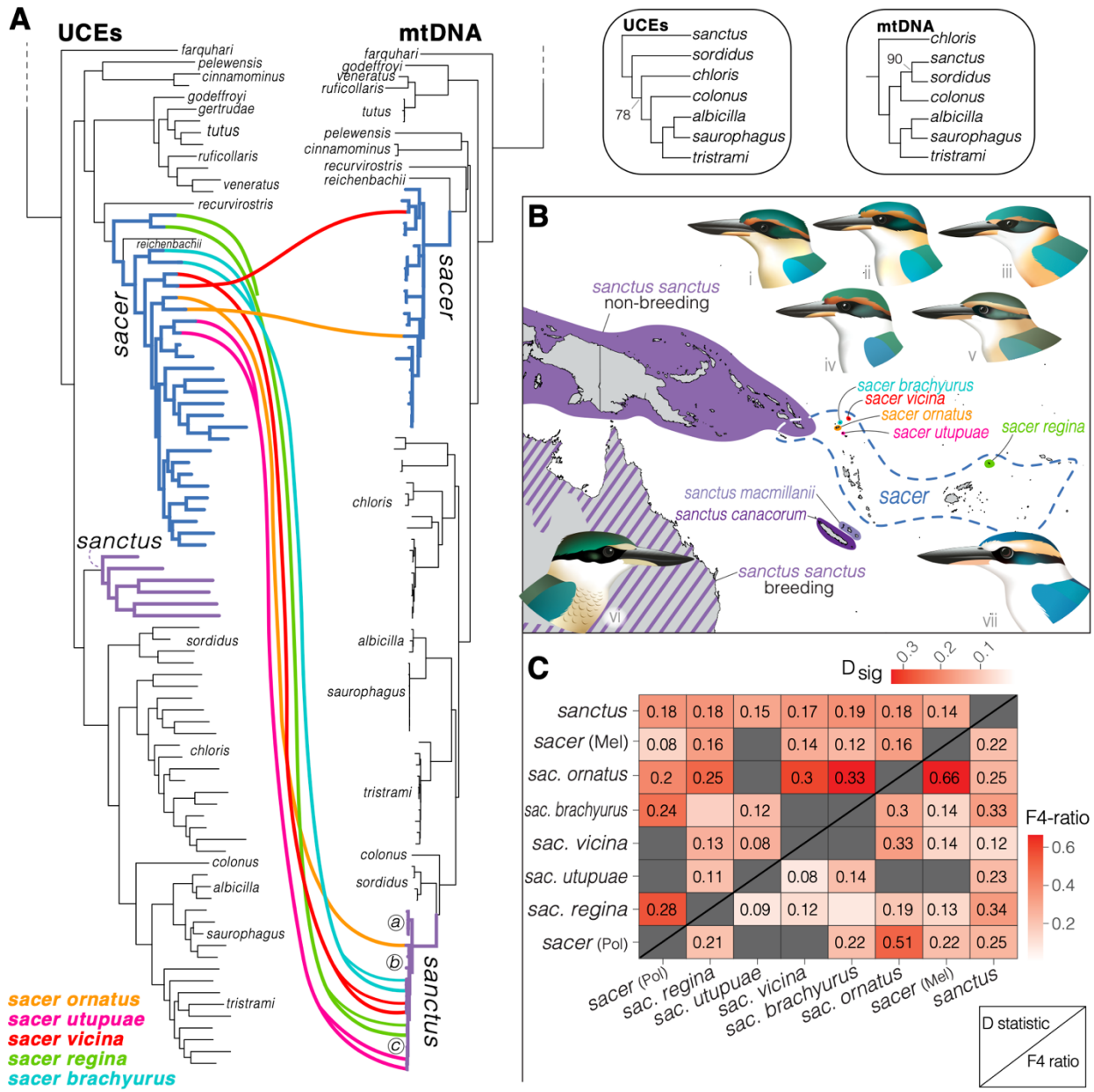

Figure 4. Evidence of gene flow and mitochondrial capture within some Pacific Kingfisher (*T. sacer*) taxa and Sacred Kingfisher (*T. sanctus*). A) Partitioned IQtree phylogenies inferred from the 90% complete UCE matrix and 13 mitochondrial genes. Note that the mtDNA phylogeny for the Australasian clade (*T. sanctus*, *T. tristrami*, and allies) is different from the UCE topology, which has been described previously (DeRaad et al. 2023). In the mtDNA phylogeny, there are two clades of *T. sanctus*: a clade of four of the five sedentary, island endemic *T. sanctus* taxa (a), which is sister to the clade comprising the migratory and nominate taxon *T. sanctus sanctus* (b), the five *T. sacer* taxa (colored lines), and the fifth

island endemic sedentary taxon *T. sanctus macmillani* (c). See Fig. S19 for tip labels. B) Range map of both species, highlighting the subspecific ranges of the *T. sacer* taxa with *T. sanctus* mtDNA (see Fig. S1 for the subspecific ranges of all 22 *T. sacer* taxa). Jenna McCullough created the illustrations of kingfisher taxa; names are indicated by roman numerals next to illustrations and are as follows: i, *T. sacer brachyurus*; ii, *T. sacer vicina*; iii, *T. sacer ornatus*; iv, *T. sacer utupuae*; v, *T. sacer regina*; vi, *T. sanctus sanctus*; and vii, *T. sacer sacer* (endemic to Tonga). C) Pairwise results of ABBA-BABA tests from Dsuite, with values in comparisons with FDR-adjusted significant pairwise p values. Above the diagonal line is the most significant (D_{min}) for any pairwise comparison and below are F4-ratio values. Only a subset of all comparisons is shown here, see Figs. S20–23 for the complete set.

ornatus and the Polynesian (F4 = 0.51) and Melanesian (F4 = 0.66) clades of *T. sacer*. With conservative interpretations of these tests by considering the lowest D values between multiple comparisons (D_{min}), we still see moderate signals of gene flow between *T. sacer regina* and *T. sanctus* (D_{min} = 0.13; Fig. S21) and *T. sacer* (0.16) in the species-level dataset (Fig. S21). When *T. sacer* taxa that have *T. sanctus* mtDNA are treated as their own tips, we see statistically significant signatures of gene flow between *T. sanctus* and *T. sacer brachyurus* (D_{min} = 0.08; Fig. S19) and between *T. sacer brachyurus* and *T. sacer ornatus* (D_{min} = 0.27). Long swaths of statistically significant and high D-statistic values for every species comparison, such as those shown for *T. colonus,* members of the *leucopygius* and east Polynesian clades (Fig. S21), could reflect either ancient introgression (Fig. S18), incorrect topology, or substitution rate variation caused by bottlenecked populations (Table S4, (Frankel and Ané 2023; Koppetsch et al. 2024).

Network analyses with SNaQ also confirm the presence of hybrid lineages across *Todiramphus* and explain topological discordance across datasets, with the best overall network recovering four hybrid lineages (Fig. S18C). Reticulation events for our best SNaQ topology

558 indicated that between 2–37% of the sampled genome (gamma, γ) was exchanged in each event,
559 with 1-γ being the contribution of the other parental lineage. We inferred an ancient
560 hybridization event that exchanged a sizable portion of the sampled genome between *T.*
561 *pyrrhopygius* and the ancestor of *T. australasia* + the rest of *Todiramphus* (γ = 0.378).
562 Additionally, we inferred a reticulation event between *T. farquhari* and the ancestor of the east
563 Polynesian clade (γ = 0.236), between *T. chloris* and *T. sordidus* (γ = 0.233), and very low
564 percentage of the sampled genome between *T. sanctus* and the ancestor to the other members of
565 the Australasian clade (γ = 0.022). The other best trees in the two other subsets showed similar
566 patterns of reticulation events with varying levels of γ (Fig. S18). The best inferred networks for
567 other quartet subsets inferred similar and complicated reticulation histories across *Todiramphus*,
568 including branches involving the *T. pyrrhopygius* and the *T. leucopygius* clade, as well as
569 between *T. sanctus*, *T. chloris*, and *T. sordidus.*
570
571 *Relationships within species complexes*
572 We found several cases in which *Todiramphus* species complexes do not accurately reflect
573 taxonomic groupings. First, we found that the Talaud Kingfisher (*T. enigma*, endemic to the
574 Talaud islands between Sulawesi and the Philippines), is consistently recovered within the
575 Collared Kingfisher (*T. chloris*) clade. It was most frequently supported as sister to nominate *T.*
576 *chloris* (*T. c. chloris*, endemic to Wallacea; Figs. 1, 4, S1, S8, S13, S16). Additionally, we
577 consistently found that the two most northern taxa of the *T. sacer* complex, *T. sacer pavuvu*
578 (Pavuvu I.) and *T. sacer mala* (Malita I.) of the central Solomon Islands, were embedded within
579 *T. tristrami* and closely associated with their geographically closest neighbor, *T. tristrami alberti*
580 (main chain of the Solomons Archipelago). We found that the two unnamed *T. sacer* taxa, those

from Tucopia Island in the Temotu Province of the Solomon Islands and Anietyum Island in southern Vanuatu, did not group with their assumed subspecific assignment. We never recovered a sister relationship between samples from Tucopia and representatives from its long-assumed subspecies, *T. sacer torresianus,* or between samples from Anietyum and its presumed subspecies, *T. sacer erromangae* (Mayr 1931; Gill et al. 2024; Peters 1945).

DISCUSSION

As we can efficiently sequence larger and more thoroughly sampled phylogenomic datasets, it is increasingly clear that the evolutionary histories of rapid radiations are complex (Jarvis et al. 2014; Prum et al. 2015; Malinsky et al. 2018; Zink and Vázquez-Miranda 2019; Rota et al. 2022; Mirarab et al. 2024; Stiller et al. 2024). Here, we show that whole genome resequencing of a thoroughly sampled taxonomic dataset of all described forms of a genus of 'Great Speciators' has revealed evidence of pervasive gene flow that occurred throughout its rapid radiation. We inferred deep reticulation events as well as more shallow cases of gene flow between both sympatric (*T. sanctus* and *T. sordidus*) and allopatric species (*T. sanctus* and *T. sacer*; Figs. 4, S18–22). This inferred gene flow, in concert with many rapid speciation events that precluded gene coalescence and explains the topological discordance across the four data types used in this study (UCEs, BUSCOs, SNPs, and mtDNA).

Our results confirm past work showing mitochondrial discordance in the Australasian *Todiramphus* clade (DeRaad et al. 2023) and also reveal novel signatures of gene flow with a larger and more comprehensive dataset (Figs. S19–22). Moreover, we uncovered new cases of mitochondrial discordance (Fig. 4) between *T. sanctus* and several *T. sacer* populations that nuclear data inferred as some of the earliest branches within *T. sacer*. Though our limited

604 sampling of a single individual for most taxa precluded us from more detailed population-level
605 analyses, we found signatures of gene flow between *T. sanctus* and Temotu *T. sacer* that have *T.*
606 *sanctus* mtDNA (Figs. S19–22). The inference of these hybrid lineages as divergent and non-
607 monophyletic lineages suggests that they follow the 'artefactual branch effect' (Chan et al.
608 2020b, 2023; Pyron et al. 2022). Our results suggest that there are numerous violations of the
609 traditional bifurcating species tree model within *Todiramphus* kingfishers. A next step towards
610 understanding interspecies relationships would be a sliding window approach to determine if
611 particular genomic regions are disproportionately driving the levels of discordance observed
612 here, as has been shown in early branches of Neoaves (Mirarab et al. 2024; Stiller et al. 2024).
613

614 *Gene flow within* Todiramphus *kingfishers*

615 Studies that employ genome-wide data are increasingly demonstrating the prevalence of gene
616 flow during periods of rapid diversification (Edelman et al. 2019; Taylor and Larson 2019; Guo
617 et al. 2022; Ocampo et al. 2022; Jensen et al. 2023; Jiang et al. 2024; Stiller et al. 2024; Zhao et
618 al. 2024). Here, we uncovered novel patterns of gene flow between *Todiramphus* kingfishers as
619 they rapidly diversified over the last 10 Ma. Recent population-level studies that employed either
620 mitochondrial (O'Connell et al. 2019) or RAD-seq data (DeRaad et al. 2023) did not find
621 signatures of gene flow between *T. sanctus* and other members of the Australasian clade (*T.*
622 *chloris*, *T. sordidus*, *T. colonus*, etc.). Here, comparisons between these lineages showed
623 relatively lower signatures of gene flow than other pairwise comparisons, such as between *T.*
624 *sanctus* and *T. sacer,* and within the *T. sacer* complex (Figs. S20–23). Network analyses inferred
625 a very low percentage of the sampled genome (2.2%) shared between *T. sanctus* and the ancestor
626 to the remaining members of the Australasian clade (Fig. S18). This novel inference of gene flow

627 was likely missed in prior studies due to the ever-growing size and scope of molecular datasets
628 brought to bear on this group (three mtDNA genes for O'Connell et al. 2019 vs. ~2,000 SNPs for
629 Deraad et al. 2023 vs. >85K SNPs and thousands of gene trees for this study). We are not the
630 first to uncover gene flow within Indo-Pacific kingfishers. Studies that employ phylogenomic
631 data showed persistent gene flow but maintenance of species-boundaries between the two
632 sympatric *Syma* species (sister genus to *Todiramphus*) across an elevational gradient in New
633 Guinea (Linck et al. 2020) as well as across *Ceyx,* the other 'Great Speciator' kingfisher genus
634 (Lim et al. 2010; Andersen et al. 2013; Shakya et al. 2023). Overall, our study fits into a larger
635 picture of gene flow between island endemic avian lineages, including within Fijian groups such
636 as honeyeaters and bush-warblers (Gyllenhaal et al. 2020; Mapel et al. 2021) and Indonesian
637 monarch flycatchers (Andersen et al. 2021).

638 Many of the contemporary patterns of gene flow that we observed in this study involve
639 one species in particular, the Sacred Kingfisher *T. sanctus*. Because we had limited sampling per
640 taxon, we could not pursue more detailed tests of gene flow between *T. sanctus* and other
641 species, such as Admixture (Alexander et al. 2009) or fastsimcoal2 (Excoffier et al. 2021).
642 However, observed mitochondrial discordance of five *T. sacer* taxa (*regina*, *ornatus, utupuae*,
643 *vicina*, and *brachyurus;* Fig. 4) and elevated estimates of D_{min} between *T. sanctus* and *T. sacer*
644 from ABBA-BABA tests (Figs. S19, S21) confirms the presence of gene flow. Moreover, one of
645 these *T. sacer* lineages (*regina*) is fully supported in the *T. sanctus* clade in one phylogeny
646 (BUSCO IQtree; Fig. S16). *Todiramphus sanctus* is notable because it is one of two truly
647 migratory *Todiramphus* species alongside the Forest Kingfisher (*T. macleayii*; Woodall 2001).
648 Moreover, only the nominate subspecies of *T. sanctus* is known to be migratory—the other four
649 taxa within this complex are considered sedentary and endemic to separate Pacific islands (Fig.

650 S1). We inferred gene flow between *T. sanctus* and Torresian Kingfisher (*T. sordidus*), a species
651 that also breeds in Australia. However, during its non-breeding season, *T. sanctus* occupies a
652 wide swath of the Indo-Pacific: from as far west as Sumatra, across Wallacea, New Guinea, and
653 northern Melanesia, and as far east as Makira in the Solomon Islands (Fry et al. 1992; Woodall
654 2001). Therefore, in the non-breeding season, *T. sanctus* is sympatric with upwards of 42
655 *Todiramphus* taxa (representing 15 species), compared to only five taxa (3 species) in the
656 breeding season. However, the *T. sacer* taxa that we found to have *T. sanctus* mtDNA are not
657 sympatric with wintering *T. sanctus*, as there are no records of *T. sanctus* in Temotu Province,
658 Solomon Islands, or even as far east as Wallis and Futuna (*T. sacer regina*; see Appendix 2 for
659 more details on breeding records of *T. sanctus*). This suggests a complicated history of island
660 colonization, historical gene flow, and range contraction between these two species.

661 With the lack of substantial breeding records of *T. sanctus* outside of Australia, we are
662 left with one central question: why do we infer gene flow between *T. sanctus* and Temotu *T.*
663 *sacer* (*ornatus, utupuae*, *vicina*, and *brachyurus)* and *T. s. regina* (Fig. 4) when we do not have
664 sympatric records (breeding or otherwise) of these taxa? Notably, the only islands that sedentary
665 *T. sanctus* inhabit are conspicuously void of *T. sacer*. Geographically, the closest breeding *T.*
666 *sanctus* taxon to an island with *T. sacer* is *T. sanctus macmillani* (Loyalty Islands) and the
667 undescribed *T. sacer* population on Anietyum [also written as Anatom], approximately ~220 km
668 apart. *Todiramphus sanctus macmillani* is notable because it was placed in the mitochondrial
669 clade with the migratory *T. sanctus sanctus* and all five *T. sacer* (Fig. 4). This pattern of non-
670 overlapping breeding ranges of sedentary *T. sanctus* and *T. sacer* parallels a pattern described by
671 Mayr (1932b) for Fijian whistlers (*Pachycephala*) in which the archipelago was first colonized
672 by one group and then replaced by another, forming hybrid populations as the second wave of

colonists swept through the archipelago. Notably, crown *T. sanctus* predates that for *T. sacer* (McCullough et al. 2019, McCullough et al. *in prep*), so perhaps the ancestral range of *T. sanctus* had more widespread sedentary populations across the South Pacific prior to members of the Oceanic clade's back colonization from Eastern Polynesia towards Melanesia. This hypothesis needs further testing, but it would explain the evidence of hybridization (Fig. 4) without the contemporary presence of *T. sanctus* in the areas where *T. sacer* lineages possess *T. sanctus* mtDNA.

Other sources of topological discordance

In addition to the demonstrated gene flow across the *Todiramphus* radiation (Fig. 4), topological discordance could also be attributed to other biological and methodological factors. Incomplete lineage sorting (ILS) is a well-known and pervasive source of topological discordance, especially within rapid radiations (Suh et al. 2015; Lopes et al. 2020). However, teasing apart the relative contribution of gene flow versus ILS is difficult. DeRaad et al. (2023) suggested that mitonuclear discordance within the Australasian *Todiramphus* clade was driven largely by ILS rather than nuclear gene flow or mitochondrial capture, based on largely non-significant pairwise comparisons of the ABBA-BABBA D-statistic. Here, gene and site concordance factors (gCF/sCF) between major *Todiramphus* topologies similarly suggest that ILS is likely a significant source of topological conflict across the entire genus (Fig. 3). However, ancient reticulation events consistently inferred in similar areas of the tree (Fig S18) and significant pairwise D-statistic comparisons using our comprehensive SNP dataset (Figs. S20–23), together suggest that ongoing gene flow during diversification contributed to signals of genome-wide discordance in the Austalasian clade (Figs. 2–3). While DeRaad et al. (2023) rejected

696 mitochondrial capture within the Australasian *Todiramphus* clade, our expanded taxonomic
697 sampling across the genus reveals clear cases of mitochondrial capture of recently derived *T.*
698 *sanctus* haplotypes in multiple *T. sacer* lineages, highlighting the overall complexity of the
699 heterogeneous evolutionary processes simultaneously contributing to generate the patterns of
700 relatedness we observe among extant *Todiramphus* lineages.

701 Alternatively, methodological explanations like the source (tissue or toepad) or type of
702 DNA (exonic vs. intronic) could also explain some of the topological discordance among data
703 types and tree building methods. Because our dataset relied heavily on toepad samples, we took
704 additional steps at all levels of this study to ameliorate the effects of degraded DNA on
705 topological inference. In addition to special wet lab processing of toepad-sourced genomes, we
706 performed additional UCE alignment cleaning (Smith et al. 2020) and novel methods of *in silico*
707 BUSCO extractions (see Appendix 2). Moreover, we explored filtering approaches for MSC tree
708 building methods. ASTRAL is known to perform poorly when input gene trees are built from
709 short alignments of uninformative loci (Mirarab 2023), a pervasive issue for datasets utilizing
710 degraded DNA samples from museum specimens (Andersen et al. 2019; Salter et al. 2019, 2022;
711 Smith et al. 2020; Roycroft et al. 2021; Huynh et al. 2023). For datasets that have a high degree
712 of ancient or historical samples, there is often an artefactual pattern in which high quality and
713 historical samples form distinct clusters (Fig. S2) rather than being uniformly distributed in the
714 species tree. Before filtering for parsimony informative (PI) sites, ASTRAL-inferred species
715 trees showed a clear artefactual pattern of toepad-sourced samples clustering at the base of their
716 respective species-complexes (Figs. S2, S4). This pattern disappeared when we analyzed smaller
717 sets of gene trees based on alignments with more PI sites (Figs. S11, S15). Although filtering
718 based on informativeness can introduce bias (Musher et al. 2019; Burbrink et al. 2020), the

719 approach has been used with success elsewhere (e.g., Chan et al. 2020a; Leite et al. 2021;
720 Forthman et al. 2022). We preferred it here because it is a general approach to deal with these
721 issues rather than clade-specific filtering approaches (Chen et al. 2018) or by dropping important
722 tips represented by toepads. Additionally, the clades that represented the most topological
723 discordance were from those represented by high-quality tissues (i.e., *T. farquhari*, *T.*
724 *pyrrhopygius*) or were in clades with relatively few toepad-sourced samples (i.e., the *leucopygius*
725 clade, *T. sordidus*; Fig. 2).

726 The type of DNA from which molecular markers are derived (i.e., exonic vs. intronic
727 regions) could also contribute to conflicting topological patterns. UCEs are largely sourced from
728 intronic and non-coding regions of the genome whereas BUSCOs are all exonic markers from
729 coding regions. The difference in selective pressures and therefore rates of fixed mutations, has
730 been shown to have a substantial impact in the overall topology inferred by these markers, such
731 as in higher-level phylogenomic studies of all birds (Jarvis et al. 2014; Prum et al. 2015; Reddy
732 et al. 2017). Yet, we generally find that these data types produce largely similar topologies (Figs.
733 2–3). Though less commonly used in species-level relationships of birds, these molecular
734 markers are more widely used to infer phylogenies outside of birds, such as in plants (Timilsena
735 et al. 2022; Walden and Schranz 2023), fungi (Kanzi et al. 2020), arthropods (Dias et al. 2020;
736 Van Damme et al. 2022).

737

738 *Taxonomic recommendations*

739 In line with a growing body of work that has uncovered unsuspected species-level diversity in
740 geographic radiations across the Indo-Pacific (Andersen et al. 2013; Reeve et al. 2023; Pedersen
741 et al. 2018; Irestedt et al. 2013), we too found that some taxa in our dataset require taxonomic

742 revisions based on their novel systematic relationships (see Appendix 2 for further discussion).
743 Roughly half of the *Todiramphus* diversity we sampled has never been included in a molecular
744 phylogenetic analysis. Many newly added taxa fall within their presumed species groups, such as
745 all of the subspecific diversity within *T. tristrami* (Fig. 1), but there are some instances that
746 require taxonomic changes. When Ernst Mayr described geographic variation of kingfishers
747 across the Pacific, he noted that two populations on Tucopia (Temotu Province, Solomon
748 Islands) and Aneityum (Tafea Province, Vanuatu) islands were each phenotypically distinct from
749 those on nearby islands, but he refrained from naming these as subspecies (Mayr 1931b). He
750 wrote of the birds from Anietyum, they were "indistinguishable from typical *juliae*… only the
751 distribution keeps me, for the present, from uniting it immediately with *juliae*" (Mayr 1931b, pg
752 4). To our eyes, Aneityum *sacer* are more similar to those in central Vanuatu (*T. sacer juliae*)
753 with white underparts and collar rather than the buffy *T. s. tannensis* on Tanna Island. However,
754 instead of considering this a separate taxon or grouping this population with the closest island
755 (Tanna), Aneityum birds have long been considered as part of *T. sacer erromangae*, forming a
756 curious leapfrog distribution of white-bellied birds (*erromangae* and the Aneityum form)
757 sandwiching buffy-bellied birds (Tanna). We would expect that if Aneityum birds are indeed part
758 of *T. s. erromangae* or *tannensis*, our genetic samples would be closely associated with one of
759 these taxa. For the samples from Tucopia, Mayr refrained from naming these birds as a
760 subspecific taxon because their plumages were "too worn" (Mayr 1931b), and they have been
761 considered either a part of *T. s. torresianus* (Banks Is., Vanuatu) or *T. s. melanodera* (Vanikolo
762 in Temotu Province). Whereas we sometimes found Aneityum *sacer* grouping in a subclade with
763 *T. s. erromangae* or *tannensis* and Tucopia *sacer* (Fig. 1), we never recovered Aneityum *sacer* or
764 Tucopia *sacer* as sister to either of their presumed subspecies. We suspect these could represent

independent lineages from their long-presumed subspecies but we defer naming these two populations as subspecies at this time.

CONCLUSIONS

Geographic radiations across the Indo-Pacific have been critical to the development of influential speciation theories, with genome-scale datasets providing new and accelerated insights into the complicated evolutionary histories of such rapidly diversifying clades. In this study we show that whole genome resequencing and complete sampling of a rapid radiation of mostly island kingfishers does not outright resolve the evolutionary relationships of the group. Instead, we found that four types of data (UCEs, BUSCOs, SNPs, and mtDNA) and tree building methods (ML, MSC, networks) did not infer a single well-supported and concordant species-level topology. Phylogenetic network analyses suggest that ancient introgression is likely the cause of these topological differences. The discovery of several *T. sacer* populations falling in the mitochondrial clade of a widespread and migratory taxon, *T. sanctus*, and the inference of gene flow between them ABBA-BABA tests, suggests a potential historical hybrid zone between these two species as islands were successively colonized. We were only able to pick up on these signals of hybridization because we thoroughly sampled all described diversity within the genus by relying on a sizable number of toepad-sourced data. Future studies that investigate rapid radiations in this region should incorporate widespread taxonomic and population level sampling, while also sampling large amounts of genetic data to tease apart the interacting effects of gene flow and incomplete lineage sorting on complex evolutionary histories.

ACKNOWLEDGEMENTS

This study unequivocally would not have been possible if not for the countless people since 1887 who have dedicated their time to collecting, preparing, preserving, and loaning bird specimens and their associated tissues to the world's scientists. Nearly 30% of our sampling was from the American Museum of Natural History's Whitney South Seas Expedition (1920–1941), therefore we would like to acknowledge some of its most prolific collectors: Hannibal Hamlin, Rollo H. Beck, William F. Coultas, and Ernst Mayr. We specifically thank the curators and collections managers of the American Museum of Natural History, Australian National Wildlife Collection, Charles R. Conner Museum, Delaware Museum of Natural History, the Field Museum, University of Kansas Biodiversity Institute and Natural History Museum, the Natural History Museum in London, Natural History Museum of Los Angeles County, Louisiana State University Museum of Natural Science, Museum of Comparative Zoology, Natural History Museum of Geneva, Museum of Southwestern Biology, Museum of Vertebrate Zoology, New York State Museum, Smithsonian National Zoological Park, University of Michigan Museum of Zoology, United States National Museum, University of Washington Burke Museum, Western Australia Museum, and Yale Peabody Museum. We thank Devon DeRaad, Ethan Gyllenhaal, David Tan, Fernando Machado-Stredel, Rob Lanfear, Laura Kubatko, David Bryant, Leo Joseph, and Nathan Kolbow for helpful discussions on the analyses presented in this manuscript. We would like to thank the UNM Center for Advanced Research Computing, supported in part by the National Science Foundation (NSF), for providing the research computing resources used in this work. This study was funded by NSF (DEB 2112467 to C.E.M., S.J.H., and M.J.A) and the following sources to J.M.M.: the American Museum of Natural History Frank Chapman Research Grant, UNM Biology Department Alvin R. and Caroline G. Grove Research and Richard B. Forbes Conservation awards, British Ornithologists' Union Small Ornithological

Research Grant, and the American Ornithological Society Werner and Hildegard Hesse Research award.

DATA AVAILABILITY

Supplementary material, including alignments, tree figures, and other information (supplementary methods, discussion, figures, and tables) are available in the Dryad data repository (available upon acceptance). Raw read data sequenced for this project is available on Genbank (accession upon acceptance).

APPENDICES

Appendix 1: Combined excel spreadsheet that includes five supplementary tables.

Appendix 2: Combined PDF of supplementary methods, discussion, and figures.

LITERATURE CITED

Aguillon S.M., Walsh J., Lovette I.J. 2021. Extensive hybridization reveals multiple coloration genes underlying a complex plumage phenotype. Proc. Biol. Sci. 288:20201805.

Alaei Kakhki N., Schweizer M., Lutgen D., Bowie R.C.K., Shirihai H., Suh A., Schielzeth H., Burri R. 2023. A Phylogenomic Assessment of Processes Underpinning Convergent Evolution in Open-Habitat Chats. Mol. Biol. Evol. 40.

Alexander D.H., Novembre J., Lange K. 2009. Fast model-based estimation of ancestry in unrelated individuals. Genome Res. 19:1655–1664.

Allio R., Schomaker-Bastos A., Romiguier J., Prosdocimi F., Nabholz B., Delsuc F. 2020. MitoFinder: Efficient automated large-scale extraction of mitogenomic data in target

enrichment phylogenomics. Mol. Ecol. Resour. 20:892–905.

Andersen M.J., Hosner P.A., Filardi C.E., Moyle R.G. 2015a. Phylogeny of the monarch flycatchers reveals extensive paraphyly and novel relationships within a major Australo-Pacific radiation. Mol. Phylogenet. Evol. 83:118–136.

Andersen M.J., McCullough J.M., Friedman N.R., Townsend Peterson A., Moyle R.G., Joseph L., Nyári Á.S. 2019. Ultraconserved elements resolve genus-level relationships in a major Australasian bird radiation (Aves: Meliphagidae). Emu - Austral Ornithology. 119:218–232.

Andersen M.J., McCullough J.M., Gyllenhaal E.F., Mapel X.M., Haryoko T., Jønsson K.A., Joseph L. 2021. Complex histories of gene flow and a mitochondrial capture event in a nonsister pair of birds. Mol. Ecol. 30:2087–2103.

Andersen M.J., McCullough J.M., Mauck W.M., Smith B.T., Moyle R.G. 2018. A phylogeny of kingfishers reveals an Indomalayan origin and elevated rates of diversification on oceanic islands. J. Biogeogr. 45:269–281.

Andersen M.J., Nyári Á.S., Mason I., Joseph L., Dumbacher J.P., Filardi C.E., Moyle R.G. 2014. Molecular systematics of the world's most polytypic bird: the Pachycephala pectoralis/melanura (Aves: Pachycephalidae) species complex. Zool. J. Linn. Soc. 170:566–588.

Andersen M.J., Oliveros C.H., Filardi C.E., Moyle R.G. 2013. Phylogeography of the Variable Dwarf-Kingfisher *Ceyx Lepidus* (Aves: Alcedinidae) inferred from mitochondrial and nuclear DNA sequences. Auk. 130:118–131.

Andersen M.J., Shult H.T., Cibois A., Thibault J.-C., Filardi C.E., Moyle R.G. 2015b. Rapid diversification and secondary sympatry in Australo-Pacific kingfishers (Aves: Alcedinidae: Todiramphus). R Soc Open Sci. 2:140375.

857 Bagley J.C., Uribe-Convers S., Carlsen M.M., Muchhala N. 2020. Utility of targeted sequence
858 capture for phylogenomics in rapid, recent angiosperm radiations: Neotropical Burmeistera
859 bellflowers as a case study. Mol. Phylogenet. Evol. 152:106769.
860 Baldwin B.G., Sanderson M.J. 1998. Age and rate of diversification of the Hawaiian silversword
861 alliance (Compositae). Proceedings of the National Academy of Sciences. 95:9402–9406.
862 Baum D.A. 2007. Concordance trees, concordance factors, and the exploration of reticulate
863 genealogy. Taxon. 56:417–426.
864 Baum D.A., Futuyma D.J., Hoekstra H.E., Lenski R.E., Moore A.J., Peichel C.L., Schluter D.,
865 Whitlock M.C. 2017. The Princeton Guide to Evolution. Princeton University Press.
866 Benjamini Y., Hochberg Y. 1995. Controlling the false discovery rate: A practical and powerful
867 approach to multiple testing. J. R. Stat. Soc. 57:289–300.
868 Bezanson J., Edelman A., Karpinski S., Shah V.B. 2017. Julia: A Fresh Approach to Numerical
869 Computing. SIAM Rev. 59:65–98.
870 Billerman S.M., Walsh J. 2019. Historical DNA as a tool to address key questions in avian
871 biology and evolution: A review of methods, challenges, applications, and future directions.
872 Mol. Ecol. Resour. 19:1115–1130.
873 Bolger A.M., Lohse M., Usadel B. 2014. Trimmomatic: a flexible trimmer for Illumina sequence
874 data. Bioinformatics. 30:2114–2120.
875 Broad Institute. 2019. Picard toolkit. Broad Institute, GitHub repository.
876 Bryant D., Moulton V. 2004. Neighbor-net: an agglomerative method for the construction of
877 phylogenetic networks. Mol. Biol. Evol. 21:255–265.
878 Burbrink F.T., Grazziotin F.G., Pyron R.A., Cundall D., Donnellan S., Irish F., Keogh J.S.,
879 Kraus F., Murphy R.W., Noonan B., Raxworthy C.J., Ruane S., Lemmon A.R., Lemmon

E.M., Zaher H. 2020. Interrogating Genomic-Scale Data for Squamata (Lizards, Snakes, and Amphisbaenians) Shows no Support for Key Traditional Morphological Relationships. Syst. Biol. 69:502–520.

Campbell C.R., Poelstra J.W., Yoder A.D. 2018. What is Speciation Genomics? The roles of ecology, gene flow, and genomic architecture in the formation of species. Biol. J. Linn. Soc. Lond. 124:561–583.

Capella-Gutiérrez S., Silla-Martínez J.M., Gabaldón T. 2009. trimAl: a tool for automated alignment trimming in large-scale phylogenetic analyses. Bioinformatics. 25:1972–1973.

Chan K.O., Hutter C.R., Wood P.L. Jr, Grismer L.L., Brown R.M. 2020a. Larger, unfiltered datasets are more effective at resolving phylogenetic conflict: Introns, exons, and UCEs resolve ambiguities in Golden-backed frogs (Anura: Ranidae; genus Hylarana). Mol. Phylogenet. Evol. 151:106899.

Chan K.O., Hutter C.R., Wood P.L. Jr, Grismer L.L., Das I., Brown R.M. 2020b. Gene flow creates a mirage of cryptic species in a Southeast Asian spotted stream frog complex. Mol. Ecol. 29:3970–3987.

Chan K.O., Mulcahy D.G., Anuar S. 2023. The Artefactual Branch Effect and Phylogenetic Conflict: Species Delimitation with Gene Flow in Mangrove Pit Vipers (Trimeresurus purpureomaculatus-erythrurus Complex). Syst. Biol. 72:1209–1219.

Chapman F.M. 1935. THE WHITNEY SOUTH SEA EXPEDITION. Science. 81:95–97.

Chen D., Braun E.L., Forthman M., Kimball R.T., Zhang Z. 2018. A simple strategy for recovering ultraconserved elements, exons, and introns from low coverage shotgun sequencing of museum specimens: Placement of the partridge genus Tropicoperdix within the galliformes. Mol. Phylogenet. Evol. 129:304–314.

903 Chernomor O., von Haeseler A., Minh B.Q. 2016. Terrace Aware Data Structure for
904 Phylogenomic Inference from Supermatrices. Syst. Biol. 65:997–1008.
905 Chifman J., Kubatko L. 2014. Quartet inference from SNP data under the coalescent model.
906 Bioinformatics. 30:3317–3324.
907 Clements J.F., Rasmussen P.C., Schulenberg T.S., Iliff M.J., Fredericks T.A., Gerbracht J.A.,
908 Lepage D., Spencer A., Billerman S.M., Sullivan B.L., Wood C.L. The eBird/Clements
909 checklist of Birds of the World: v2023b. Available from
910 https://www.birds.cornell.edu/clementschecklist/download/.
911 Danecek P., Bonfield J.K., Liddle J., Marshall J., Ohan V., Pollard M.O., Whitwham A., Keane
912 T., McCarthy S.A., Davies R.M., Li H. 2021. Twelve years of SAMtools and BCFtools.
913 Gigascience. 10.
914 Danecek P., McCarthy S.A. 2017. BCFtools/csq: haplotype-aware variant consequences.
915 Bioinformatics. 33:2037–2039.
916 Darwin C. 1859. On the Origin of Species . .
917 Degnan J.H., Salter L.A. 2005. Gene tree distributions under the coalescent process. Evolution.
918 59:24–37.
919 DeRaad D.A., McCullough J.M., DeCicco L.H., Hime P.M., Joseph L., Andersen M.J., Moyle
920 R.G. 2023. Mitonuclear discordance results from incomplete lineage sorting, with no
921 detectable evidence for gene flow, in a rapid radiation of Todiramphus kingfishers. Mol.
922 Ecol.
923 Dias G.R., Dupim E.G., Vanderlinde T., Mello B., Carvalho A.B. 2020. A phylogenomic study
924 of Steganinae fruit flies (Diptera: Drosophilidae): strong gene tree heterogeneity and
925 evidence for monophyly. BMC Evol. Biol. 20:141.

Dobzhansky T. 1937. Genetics and the Origin of Species. Columbia University Press.

Durand E.Y., Patterson N., Reich D., Slatkin M. 2011. Testing for ancient admixture between closely related populations. Mol. Biol. Evol. 28:2239–2252.

Edelman N.B., Frandsen P.B., Miyagi M., Clavijo B., Davey J., Dikow R.B., García-Accinelli G., Van Belleghem S.M., Patterson N., Neafsey D.E., Challis R., Kumar S., Moreira G.R.P., Salazar C., Chouteau M., Counterman B.A., Papa R., Blaxter M., Reed R.D., Dasmahapatra K.K., Kronforst M., Joron M., Jiggins C.D., McMillan W.O., Di Palma F., Blumberg A.J., Wakeley J., Jaffe D., Mallet J. 2019. Genomic architecture and introgression shape a butterfly radiation. Science. 366:594–599.

Eliason C.M., Hains T., McCullough J., Andersen M.J., Hackett S.J. 2022. Genomic novelty within a “great speciator” revealed by a high-quality reference genome of the collared kingfisher (Todiramphus chloris collaris). G3 Genes|Genomes|Genetics. 12:jkac260.

Eliason C.M., Mellenthin L.E., Hains T., McCullough J.M., Pirro S., Andersen M.J., Hackett S.J. 2023. Genomic signatures of convergent shifts to plunge-diving behavior in birds. Commun Biol. 6:1011.

Ernst M., Jønsson K.A., Ericson P.G.P., Blom M.P.K., Irestedt M. 2022. Utilizing museomics to trace the complex history and species boundaries in an avian-study system of conservation concern. Heredity . 128:159–168.

Excoffier L., Marchi N., Marques D.A., Matthey-Doret R., Gouy A., Sousa V.C. 2021. fastsimcoal2: demographic inference under complex evolutionary scenarios. Bioinformatics. 37:4882–4885.

Faircloth B.C. 2016. PHYLUCE is a software package for the analysis of conserved genomic loci. Bioinformatics. 32:786–788.

949 Faircloth B.C., McCormack J.E., Crawford N.G., Harvey M.G., Brumfield R.T., Glenn T.C.
950 2012. Ultraconserved Elements Anchor Thousands of Genetic Markers Spanning Multiple
951 Evolutionary Timescales. Syst. Biol. 61:717–726.
952 Felsenstein J. 1978. Cases in which Parsimony or Compatibility Methods will be Positively
953 Misleading. Syst. Biol. 27:401–410.
954 Feng S., Stiller J., Deng Y., Armstrong J., Fang Q., Reeve A.H., Xie D., Chen G., Guo C.,
955 Faircloth B.C., Petersen B., Wang Z., Zhou Q., Diekhans M., Chen W., Andreu-Sánchez S.,
956 Margaryan A., Howard J.T., Parent C., Pacheco G., Sinding M.-H.S., Puetz L., Cavill E.,
957 Ribeiro Â.M., Eckhart L., Fjeldså J., Hosner P.A., Brumfield R.T., Christidis L., Bertelsen
958 M.F., Sicheritz-Ponten T., Tietze D.T., Robertson B.C., Song G., Borgia G., Claramunt S.,
959 Lovette I.J., Cowen S.J., Njoroge P., Dumbacher J.P., Ryder O.A., Fuchs J., Bunce M., Burt
960 D.W., Cracraft J., Meng G., Hackett S.J., Ryan P.G., Jønsson K.A., Jamieson I.G., da
961 Fonseca R.R., Braun E.L., Houde P., Mirarab S., Suh A., Hansson B., Ponnikas S., Sigeman
962 H., Stervander M., Frandsen P.B., van der Zwan H., van der Sluis R., Visser C.,
963 Balakrishnan C.N., Clark A.G., Fitzpatrick J.W., Bowman R., Chen N., Cloutier A.,
964 Sackton T.B., Edwards S.V., Foote D.J., Shakya S.B., Sheldon F.H., Vignal A., Soares
965 A.E.R., Shapiro B., González-Solís J., Ferrer-Obiol J., Rozas J., Riutort M., Tigano A.,
966 Friesen V., Dalén L., Urrutia A.O., Székely T., Liu Y., Campana M.G., Corvelo A.,
967 Fleischer R.C., Rutherford K.M., Gemmell N.J., Dussex N., Mouritsen H., Thiele N.,
968 Delmore K., Liedvogel M., Franke A., Hoeppner M.P., Krone O., Fudickar A.M., Milá B.,
969 Ketterson E.D., Fidler A.E., Friis G., Parody-Merino Á.M., Battley P.F., Cox M.P., Lima
970 N.C.B., Prosdocimi F., Parchman T.L., Schlinger B.A., Loiselle B.A., Blake J.G., Lim H.C.,
971 Day L.B., Fuxjager M.J., Baldwin M.W., Braun M.J., Wirthlin M., Dikow R.B., Ryder

T.B., Camenisch G., Keller L.F., DaCosta J.M., Hauber M.E., Louder M.I.M., Witt C.C., McGuire J.A., Mudge J., Megna L.C., Carling M.D., Wang B., Taylor S.A., Del-Rio G., Aleixo A., Vasconcelos A.T.R., Mello C.V., Weir J.T., Haussler D., Li Q., Yang H., Wang J., Lei F., Rahbek C., Gilbert M.T.P., Graves G.R., Jarvis E.D., Paten B., Zhang G. 2021. Author Correction: Dense sampling of bird diversity increases power of comparative genomics. Nature. 592:E24.

Forthman M., Braun E.L., Kimball R.T. 2022. Gene tree quality affects empirical coalescent branch length estimation. Zool. Scr. 51:1–13.

Frankel L.E., Ané C. 2023. Summary Tests of Introgression Are Highly Sensitive to Rate Variation Across Lineages. Syst. Biol. 72:1357–1369.

French W.M. 1957. [Correspondence] Birds of the Solomon Islands. Ibis . 99:126–127.

Fry C.H., Fry K., Harris A. 1992. Kingfishers, Bee-eaters & Rollers: A handbook. Princeton, New Jersey: Princeton University Press.

Gill F., Donsker D., Rasmussen P. 2024. IOC world bird list 14.1. Available from https://www.worldbirdnames. org/new/ioc-lists/master-list-2/.

Grant P.R., Grant B.R. 2006. Evolution of character displacement in Darwin's finches. Science. 313:224–226.

Guo W., Sun D., Cao Y., Xiao L., Huang X., Ren W., Xu S., Yang G. 2022. Extensive Interspecific Gene Flow Shaped Complex Evolutionary History and Underestimated Species Diversity in Rapidly Radiated Dolphins. J. Mamm. Evol. 29:353–367.

Gyllenhaal E.F., Mapel X.M., Naikatini A., Moyle R.G., Andersen M.J. 2020. A test of island biogeographic theory applied to estimates of gene flow in a Fijian bird is largely consistent with neutral expectations. Mol. Ecol. 29:4059–4073.

995 Hartert E. 1904. The birds of the South-west Islands, Wetter, Roma, Kisser, Letti and Moa.
996 Novitates Zoologicae. 11:174–221.
997 Hoang D.T., Chernomor O., von Haeseler A., Minh B.Q., Vinh L.S. 2018. UFBoot2: Improving
998 the Ultrafast Bootstrap Approximation. Mol. Biol. Evol. 35:518–522.
999 Huson D.H., Bryant D. 2006. Application of phylogenetic networks in evolutionary studies. Mol.
1000 Biol. Evol. 23:254–267.
1001 Huynh S., Cloutier A., Sin S.Y.W. 2023. Museomics and phylogenomics of lovebirds
1002 (Psittaciformes, Psittaculidae, Agapornis) using low-coverage whole-genome sequencing.
1003 Mol. Phylogenet. Evol. 185:107822.
1004 Irestedt M., Fabre P.H., Batalha-Filho H., Jonsson K.A., Roselaar C.S., Sangster G., Ericson
1005 P.G.P. 2013. The spatio-temporal colonization and diversification across the Indo-Pacific by
1006 a "great speciator" (Aves, Erythropitta erythrogaster). Proceedings of the Royal Society B:
1007 Biological Sciences. 280:20130309–20130309.
1008 Irestedt M., Thörn F., Müller I.A., Jønsson K.A., Ericson P.G.P., Blom M.P.K. 2022. A guide to
1009 avian museomics: Insights gained from resequencing hundreds of avian study skins. Mol.
1010 Ecol. Resour. 22:2672–2684.
1011 Jarvis E.D., Mirarab S., Aberer A.J., Li B., Houde P., Li C., Ho S.Y.W., Faircloth B.C., Nabholz
1012 B., Howard J.T., Suh A., Weber C.C., da Fonseca R.R., Li J., Zhang F., Li H., Zhou L.,
1013 Narula N., Liu L., Ganapathy G., Boussau B., Bayzid M.S., Zavidovych V., Subramanian
1014 S., Gabaldón T., Capella-Gutiérrez S., Huerta-Cepas J., Rekepalli B., Munch K., Schierup
1015 M., Lindow B., Warren W.C., Ray D., Green R.E., Bruford M.W., Zhan X., Dixon A., Li
1016 S., Li N., Huang Y., Derryberry E.P., Bertelsen M.F., Sheldon F.H., Brumfield R.T., Mello
1017 C.V., Lovell P.V., Wirthlin M., Schneider M.P.C., Prosdocimi F., Samaniego J.A., Vargas

1018 Velazquez A.M., Alfaro-Núñez A., Campos P.F., Petersen B., Sicheritz-Ponten T., Pas A.,
1019 Bailey T., Scofield P., Bunce M., Lambert D.M., Zhou Q., Perelman P., Driskell A.C.,
1020 Shapiro B., Xiong Z., Zeng Y., Liu S., Li Z., Liu B., Wu K., Xiao J., Yinqi X., Zheng Q.,
1021 Zhang Y., Yang H., Wang J., Smeds L., Rheindt F.E., Braun M., Fjeldså J., Orlando L.,
1022 Barker F.K., Jønsson K.A., Johnson W., Koepfli K.-P., O'Brien S., Haussler D., Ryder
1023 O.A., Rahbek C., Willerslev E., Graves G.R., Glenn T.C., McCormack J., Burt D., Ellegren
1024 H., Alström P., Edwards S.V., Stamatakis A., Mindell D.P., Cracraft J., Braun E.L.,
1025 Warnow T., Jun W., Gilbert M.T.P., Zhang G. 2014. Whole-genome analyses resolve early
1026 branches in the tree of life of modern birds. Science. 346:1320–1331.
1027 Jensen A., Swift F., de Vries D., Beck R.M.D., Kuderna L.F.K., Knauf S., Chuma I.S., Keyyu
1028 J.D., Kitchener A.C., Farh K., Rogers J., Marques-Bonet T., Detwiler K.M., Roos C.,
1029 Guschanski K. 2023. Complex Evolutionary History With Extensive Ancestral Gene Flow
1030 in an African Primate Radiation. Mol. Biol. Evol. 40.
1031 Jiang Z., Zang W., Ericson P.G.P., Song G., Wu S., Feng S., Drovetski S.V., Liu G., Zhang D.,
1032 Saitoh T., Alström P., Edwards S.V., Lei F., Qu Y. 2024. Gene flow and an anomaly zone
1033 complicate phylogenomic inference in a rapidly radiated avian family (Prunellidae). BMC
1034 Biol. 22:49.
1035 Kalyaanamoorthy S., Minh B.Q., Wong T.K.F., von Haeseler A., Jermiin L.S. 2017.
1036 ModelFinder: fast model selection for accurate phylogenetic estimates. Nat. Methods.
1037 14:587–589.
1038 Kanzi A.M., Trollip C., Wingfield M.J., Barnes I., Van der Nest M.A., Wingfield B.D. 2020.
1039 Phylogenomic incongruence in Ceratocystis: a clue to speciation? BMC Genomics. 21:362.
1040 Katoh K., Standley D.M. 2013. MAFFT multiple sequence alignment software version 7:

1041 improvements in performance and usability. Mol. Biol. Evol. 30:772–780.
1042 Kearns A.M., Joseph L., White L.C., Austin J.J., Baker C., Driskell A.C., Malloy J.F., Omland
1043 K.E. 2016. Norfolk Island Robins are a distinct endangered species: ancient DNA unlocks
1044 surprising relationships and phenotypic discordance within the Australo-Pacific Robins.
1045 Conserv. Genet. 17:321–335.
1046 Kelly J., Rahman A., Grass I., Tasirin J.S., Waltert M. 2017. Avifaunal status updates, range
1047 extensions and potential new taxa on the lesser Sangihe and Talaud islands, Indonesia.
1048 Raffles Bull. Zool. 65:482–496.
1049 Koppetsch T., Malinsky M., Matschiner M. 2024. Towards reliable detection of introgression in
1050 the presence of among-species rate variation. bioRxiv.:2023.05.21.541635.
1051 Korneliussen T.S., Albrechtsen A., Nielsen R. 2014. ANGSD: Analysis of Next Generation
1052 Sequencing Data. BMC Bioinformatics. 15:356.
1053 Kozlov A.M., Darriba D., Flouri T., Morel B., Stamatakis A. 2019. RAxML-NG: a fast, scalable
1054 and user-friendly tool for maximum likelihood phylogenetic inference. Bioinformatics.
1055 35:4453–4455.
1056 Kubatko L., Knowles L. 2023. Species Tree Inference: A Guide to Methods and Applications.
1057 Princeton University Press.
1058 Kuhn R.M., Haussler D., Kent W.J. 2013. The UCSC genome browser and associated tools.
1059 Brief. Bioinform. 14:144–161.
1060 Lamichhaney S., Berglund J., Almén M.S., Maqbool K., Grabherr M., Martinez-Barrio A.,
1061 Promerová M., Rubin C.-J., Wang C., Zamani N., Grant B.R., Grant P.R., Webster M.T.,
1062 Andersson L. 2015. Evolution of Darwin/’s finches and their beaks revealed by genome
1063 sequencing. Nature. 518:371–375.

1064 Landis M.J., Freyman W.A., Baldwin B.G. 2018. Retracing the Hawaiian silversword radiation
1065 despite phylogenetic, biogeographic, and paleogeographic uncertainty. Evolution. 72:2343–
1066 2359.
1067 Leite R.N., Kimball R.T., Braun E.L., Derryberry E.P., Hosner P.A., Derryberry G.E., Anciães
1068 M., McKay J.S., Aleixo A., Ribas C.C., Brumfield R.T., Cracraft J. 2021. Phylogenomics of
1069 manakins (Aves: Pipridae) using alternative locus filtering strategies based on
1070 informativeness. Mol. Phylogenet. Evol. 155:107013.
1071 Lerner H.R.L., Meyer M., James H.F., Hofreiter M., Fleischer R.C. 2011. Multilocus resolution
1072 of phylogeny and timescale in the extant adaptive radiation of Hawaiian honeycreepers.
1073 Curr. Biol. 21:1838–1844.
1074 Lieberman B.S. 2012. Adaptive Radiations in the Context of Macroevolutionary Theory: A
1075 Paleontological Perspective. Evol. Biol. 39:181–191.
1076 Li H. 2011. A statistical framework for SNP calling, mutation discovery, association mapping
1077 and population genetical parameter estimation from sequencing data. Bioinformatics.
1078 27:2987–2993.
1079 Li H., Durbin R. 2009. Fast and accurate short read alignment with Burrows-Wheeler transform.
1080 Bioinformatics. 25:1754–1760.
1081 Lim B.T.M., Sadanandan K.R., Dingle C., Leung Y.Y., Prawiradilaga D.M., Irham M., Ashari
1082 H., Lee J.G.H., Rheindt F.E. 2019. Molecular evidence suggests radical revision of species
1083 limits in the great speciator white-eye genus Zosterops. J. Ornithol. 160:1–16.
1084 Lim H.C., Sheldon F.H., Moyle R.G. 2010. Extensive color polymorphism in the southeast Asian
1085 oriental dwarf kingfisher Ceyx erithaca: a result of gene flow during population divergence?
1086 J. Avian Biol. 41:305–318.

1087 Linck E., Freeman B.G., Dumbacher J.P. 2020. Speciation and gene flow across an elevational
1088 gradient in New Guinea kingfishers. J. Evol. Biol. 33:1643–1652.
1089 Lopes F., Oliveira L.R., Kessler A., Beux Y., Crespo E., Cárdenas-Alayza S., Majluf P.,
1090 Sepúlveda M., Brownell R.L., Franco-Trecu V., Páez-Rosas D., Chaves J., Loch C.,
1091 Robertson B.C., Acevedo-Whitehouse K., Elorriaga-Verplancken F.R., Kirkman S.P., Peart
1092 C.R., Wolf J.B.W., Bonatto S.L. 2020. Phylogenomic Discordance in the Eared Seals is best
1093 explained by Incomplete Lineage Sorting following Explosive Radiation in the Southern
1094 Hemisphere. Syst. Biol. 70:786–802.
1095 Lydekker R. 1896. A Geographical History of Mammals. The University Press.
1096 MacArthur R.H., Wilson E.O. 1967. The Theory of Island Biogeography. Princeton, New Jersey:
1097 Princeton University Press.
1098 Maddison W.P., Knowles L.L. 2006. Inferring phylogeny despite incomplete lineage sorting.
1099 Syst. Biol. 55:21–30.
1100 Mahler D.L., Revell L.J., Glor R.E., Losos J.B. 2010. Ecological opportunity and the rate of
1101 morphological evolution in the diversification of Greater Antillean anoles. Evolution.
1102 64:2731–2745.
1103 Malinsky M., Matschiner M., Svardal H. 2021. Dsuite - Fast D-statistics and related admixture
1104 evidence from VCF files. Mol. Ecol. Resour. 21:584–595.
1105 Malinsky M., Svardal H., Tyers A.M., Miska E.A., Genner M.J., Turner G.F., Durbin R. 2018.
1106 Whole-genome sequences of Malawi cichlids reveal multiple radiations interconnected by
1107 gene flow. Nat Ecol Evol. 2:1940–1955.
1108 Manni M., Berkeley M.R., Seppey M., Simão F.A., Zdobnov E.M. 2021a. BUSCO Update:
1109 Novel and Streamlined Workflows along with Broader and Deeper Phylogenetic Coverage

1110 for Scoring of Eukaryotic, Prokaryotic, and Viral Genomes. Mol. Biol. Evol. 38:4647–4654.
1111 Manni M., Berkeley M.R., Seppey M., Zdobnov E.M. 2021b. BUSCO: Assessing Genomic Data
1112 Quality and Beyond. Curr Protoc. 1:e323.
1113 Mapel X.M., Gyllenhaal E.F., Modak T.H., DeCicco L.H., Naikatini A., Utzurrum R.B., Seamon
1114 J.O., Cibois A., Thibault J.-C., Sorenson M.D., Moyle R.G., Barrow L.N., Andersen M.J.
1115 2021. Inter- and intra-archipelago dynamics of population structure and gene flow in a
1116 Polynesian bird. Mol. Phylogenet. Evol. 156:107034.
1117 Marki P.Z., Fjeldså J., Irestedt M., Jønsson K.A. 2018. Molecular phylogenetics and species
1118 limits in a cryptically coloured radiation of Australo-Papuan passerine birds
1119 (Pachycephalidae: Colluricincla). Mol. Phylogenet. Evol. 124:100–105.
1120 Mayr E. 1931a. Notes on fantails of the genus Rhipidura. Am. Mus. Novit.
1121 Mayr E. 1931b. Birds collected during the Whitney South Sea Expedition 12 Notes on Halcyon
1122 chloris and some of its subspecies. Am. Mus. Novit. 469:1–10.
1123 Mayr E. 1932a. Birds collected during the Whitney South Sea Expedition. 18, Notes on
1124 Meliphagidae from Polynesia and the Solomon Islands. Am. Mus. Novit. 516:1–30.
1125 Mayr E. 1932b. Birds collected during the Whitney South Sea Expedition. 21, Notes on
1126 thickheads (*Pachycephala*) from Polynesia. American Museum novitates; no. 531.
1127 Mayr E. 1935. Birds collected during the Whitney South Sea Expedition. 30, Descriptions of
1128 twenty-five new species and subspecies. American Museum novitates; no. 820.
1129 Mayr E. 1940. Speciation phenomena in birds. Am. Nat.
1130 Mayr E. 1941. Birds collected during the Whitney South Sea Expedition. 47, Notes on the genera
1131 Halcyon, Turdus and Eurostopodus. American Museum novitates ; no. 1152. .
1132 Mayr E. 1942. Systematics and the Origin of Species. New York: Columbia University Press.

Mayr E. 1963. Animal Species and Evolution. Cambridge, Massachusetts: Belknap Press.

Mayr E., Diamond J.M. 2001. The Birds of Northern Melanesia: Speciation, Ecology, and Biogeography. New York: Oxford University Press.

McCormack J.E., Tsai W.L.E., Faircloth B.C. 2015. Sequence capture of ultraconserved elements from bird museum specimens. Mol. Ecol. Resour. 16:1189–1203.

McCullough J.M., DeCicco L.H., Herr M.W., Holland P., Pikacha D., Lavery T.H., Olson K.V., DeRaad D.A., Tigulu I.G., Mapel X.M., Klicka L.B., Famoo R., Hobete J., Runi L., Rusa G., Tippet A., Boseto D., Brown R.M., Moyle R.G., Andersen M.J. 2023. A Survey of Terrestrial Vertebrates of Tetepare Island, Solomon Islands, Including Six New Island Records1. pasc. 76:411–435.

McCullough J.M., Gyllenhaal E.F., Mapel X.M., Andersen M.J., Joseph L. 2021. Taxonomic implications of recent molecular analyses of Spectacled (Symposiachrus trivirgatus) and Spot-winged (S. guttula) Monarchs (Passeriformes: Monarchidae). Emu - Austral Ornithology. 121:365–371.

McCullough J.M., Moyle R.G., Smith B.T., Andersen M.J. 2019. A Laurasian origin for a pantropical bird radiation is supported by genomic and fossil data (Aves: Coraciiformes). Proceedings of the Royal Society B: Biological Sciences. 286:20190122.

McCullough J.M., Eliason C., Hackett S., Myers C.E., Andersen M.J. (*in prep*). Genetic drift underlies rapid plumage evolution in a rapid island radiation of ‘Great Speciators’.

McKenna A., Hanna M., Banks E., Sivachenko A., Cibulskis K., Kernytsky A., Garimella K., Altshuler D., Gabriel S., Daly M., DePristo M.A. 2010. The Genome Analysis Toolkit: a MapReduce framework for analyzing next-generation DNA sequencing data. Genome Res. 20:1297–1303.

Minh B.Q., Dang C.C., Vinh L.S., Lanfear R. 2021. QMaker: Fast and Accurate Method to Estimate Empirical Models of Protein Evolution. Syst. Biol. 70:1046–1060.

Minh B.Q., Hahn M.W., Lanfear R. 2020a. New Methods to Calculate Concordance Factors for Phylogenomic Datasets. Mol. Biol. Evol. 37:2727–2733.

Minh B.Q., Schmidt H.A., Chernomor O., Schrempf D., Woodhams M.D., von Haeseler A., Lanfear R. 2020b. IQ-TREE 2: New Models and Efficient Methods for Phylogenetic Inference in the Genomic Era. Mol. Biol. Evol. 37:1530–1534.

Mirarab S. 2023. Species Tree Estimation Using ASTRAL: Practical Considerations. In: Kubatko L.S., Knowles L.L., editors. Species Tree Inference: A Guide to Methods and Applications. Princeton University Press. p. 43–67.

Mirarab S., Rivas-González I., Feng S., Stiller J., Fang Q., Mai U., Hickey G., Chen G., Brajuka N., Fedrigo O., Formenti G., Wolf J.B.W., Howe K., Antunes A., Schierup M.H., Paten B., Jarvis E.D., Zhang G., Braun E.L. 2024. A region of suppressed recombination misleads neoavian phylogenomics. Proc. Natl. Acad. Sci. U. S. A. 121:e2319506121.

Moen D., Morlon H. 2014. Why does diversification slow down? Trends Ecol. Evol. 29:190–197.

Mo Y.K., Lanfear R., Hahn M.W., Minh B.Q. 2023. Updated site concordance factors minimize effects of homoplasy and taxon sampling. Bioinformatics. 39.

Moyle R.G. 2006. A Molecular phylogeny of Kingfishers (Alcedinidae) with insights into early biogeographic history. Auk. 123:487–413.

Moyle R.G., Filardi C.E., Smith C.E., Diamond J.M. 2009. Explosive Pleistocene diversification and hemispheric expansion of a ``great speciator''. Proc. Natl. Acad. Sci. U. S. A. 106:1863–1868.

Müller S. 1846. Ueber den Charakter der Thierwelt auf den Inseln des indischen Archipels, ein Beitrag zur zoologischen Geographie. Archiv für Naturgeschichte. 12:109–128.

Murphy N.R., Hellwig R.J. 1996. Improved nucleic acid organic extraction through use of a unique gel barrier material. Biotechniques. 21:934–6, 938–9.

Musher L.J., Catanach T.A., Valqui T., Brumfield R.T., Aleixo A., Johnson K.P., Weckstein J.D. 2024. Whole-genome phylogenomics of the tinamous (Aves: Tinamidae): comparing gene tree estimation error between BUSCOs and UCEs illuminates rapid divergence with introgression. bioRxiv.:2024.01.22.576737.

Musher L.J., Ferreira M., Auerbach A.L., McKay J., Cracraft J. 2019. Why is Amazonia a "source" of biodiversity? Climate-mediated dispersal and synchronous speciation across the Andes in an avian group (Tityrinae). Proceedings of the Royal Society B: Biological Sciences. 286:20182343.

Nacer D.F., Raposo do Amaral F. 2017. Striking pseudogenization in avian phylogenetics: Numts are large and common in falcons. Mol. Phylogenet. Evol. 115:1–6.

Nei M. 1972. Genetic distance between populations. Am. Nat. 106:283–292.

Nosil P. 2008. Speciation with gene flow could be common. Mol. Ecol. 17:2103–2106.

Ocampo D., Winker K., Miller M.J., Sandoval L., Uy J.A.C. 2022. Rapid diversification of the Variable Seedeater superspecies complex despite widespread gene flow. Mol. Phylogenet. Evol. 173:107510.

O'Connell D.P., Kelly D.J., Lawless N., Karya A., Analuddin K., Marples N.M. 2019. Diversification of a `great speciator' in the Wallacea region: differing responses of closely related resident and migratory kingfisher species (Aves: Alcedinidae: Todiramphus). Ibis . 161:806–823.

1202 Ó Marcaigh F., Kelly D.J., O'Connell D.P., Analuddin K., Karya A., McCloughan J., Tolan E.,
1203 Lawless N., Marples N.M. 2022. Small islands and large biogeographic barriers have driven
1204 contrasting speciation patterns in Indo-Pacific sunbirds (Aves: Nectariniidae). Zool. J. Linn.
1205 Soc. 198:72–92.
1206 Patterson N., Moorjani P., Luo Y., Mallick S., Rohland N., Zhan Y., Genschoreck T., Webster
1207 T., Reich D. 2012. Ancient admixture in human history. Genetics. 192:1065–1093.
1208 Pedersen B.S., Quinlan A.R. 2017. Mosdepth: quick coverage calculation for genomes and
1209 exomes. Bioinformatics. 34:867–868.
1210 Pembleton L.W., Cogan N.O.I., Forster J.W. 2013. StAMPP: an R package for calculation of
1211 genetic differentiation and structure of mixed-ploidy level populations. Mol. Ecol. Resour.
1212 13:946–952.
1213 Peters J.L. 1945. Check-list of birds of the World. Cambridge, Massachusetts: Harvard
1214 University Press.
1215 Pertea G., Pertea M. 2020. GFF Utilities: GffRead and GffCompare. F1000Res. 9.
1216 Pratt R.C., Gibb G.C., Morgan-Richards M., Phillips M.J., Hendy M.D., Penny D. 2009. Toward
1217 resolving deep neoaves phylogeny: data, signal enhancement, and priors. Mol. Biol. Evol.
1218 26:313–326.
1219 Prum R.O., Berv J.S., Dornburg A., Field D.J., Townsend J.P., Lemmon E.M., Lemmon A.R.
1220 2015. A comprehensive phylogeny of birds (Aves) using targeted next-generation DNA
1221 sequencing. Nature. 526:569–573.
1222 Pyron R.A., O'Connell K.A., Lemmon E.M., Lemmon A.R., Beamer D.A. 2022. Candidate-
1223 species delimitation in Desmognathus salamanders reveals gene flow across lineage
1224 boundaries, confounding phylogenetic estimation and clarifying hybrid zones. Ecol. Evol.

12:e8574.

de Queiroz K. 1999. The general lineage concept of species and the defining properties of the species category. In: Wilson R.A., editor. Species: New Interdisciplinary Essays. Cambridge, Massachusetts: A Bradford Book. p. 46–89.

de Quieroz K. 1998. The general lineage concept of species, species criteria, and the process of speciation. In: Howard D.J., Berlocher S.H., editors. Endless Forms: Species and Speciation. Oxford: Oxford University Press. p. 57–75.

Quinlan A.R., Hall I.M. 2010. BEDTools: a flexible suite of utilities for comparing genomic features. Bioinformatics. 26:841–842.

Rabiee M., Sayyari E., Mirarab S. 2019. Multi-allele species reconstruction using ASTRAL. Mol. Phylogenet. Evol. 130:286–296.

Raxworthy C.J., Smith B.T. 2021. Mining museums for historical DNA: advances and challenges in museomics. Trends Ecol. Evol. 36:1049–1060.

R Development Core Team. 2013. R: A language and environment for statistical computing. .

Reddy S., Kimball R.T., Pandey A., Hosner P.A., Braun M.J., Hackett S.J., Han K.-L., Harshman J., Huddleston C.J., Kingston S., Marks B.D., Miglia K.J., Moore W.S., Sheldon F.H., Witt C.C., Yuri T., Braun E.L. 2017. Why Do Phylogenomic Data Sets Yield Conflicting Trees? Data Type Influences the Avian Tree of Life more than Taxon Sampling. Syst. Biol. 66:857–879.

Reeve A.H., Gower G., Pujolar J.M., Smith B.T., Petersen B., Olsson U., Haryoko T., Koane B., Maiah G., Blom M.P.K., Ericson P.G.P., Irestedt M., Racimo F., Jønsson K.A. 2023. Population genomics of the island thrush elucidates one of earth's great archipelagic radiations. Evol Lett. 7:24–36.

1248 Riley J. 2003. Population sizes and the conservation status of endemic and restricted-range bird
1249 species on Karakelang, Talaud Islands, Indonesia. Bird Conserv. Int. 13:59–74.
1250 Riley J., Hicks D., Wardill J. 1998. The taxonomic status of Halcyon enigma on the Talaud
1251 islands, Indonesia. Bull. Am. Assoc. Hist. Nurs.
1252 Rohland N., Harney E., Mallick S., Nordenfelt S., Reich D. 2015. Partial uracil–DNA–
1253 glycosylase treatment for screening of ancient DNA. Philos. Trans. R. Soc. Lond. B Biol.
1254 Sci. 370:20130624.
1255 Rota J., Twort V., Chiocchio A., Peña C., Wheat C.W., Kaila L., Wahlberg N. 2022. The
1256 unresolved phylogenomic tree of butterflies and moths (Lepidoptera): Assessing the
1257 potential causes and consequences. Syst. Entomol. 47:531–550.
1258 Roycroft E.J., Moussalli A., Rowe K.C. 2020. Phylogenomics Uncovers Confidence and
1259 Conflict in the Rapid Radiation of Australo-Papuan Rodents. Syst. Biol. 69:431–444.
1260 Roycroft E., MacDonald A.J., Moritz C., Moussalli A., Portela Miguez R., Rowe K.C. 2021.
1261 Museum genomics reveals the rapid decline and extinction of Australian rodents since
1262 European settlement. Proc. Natl. Acad. Sci. U. S. A. 118.
1263 Roycroft E., Moritz C., Rowe K.C., Moussalli A., Eldridge M.D.B., Portela Miguez R., Piggott
1264 M.P., Potter S. 2022. Sequence Capture From Historical Museum Specimens: Maximizing
1265 Value for Population and Phylogenomic Studies. Frontiers in Ecology and Evolution. 10.
1266 Rundell R.J., Price T.D. 2009. Adaptive radiation, nonadaptive radiation, ecological speciation
1267 and nonecological speciation. Trends Ecol. Evol. 24:394–399.
1268 Salter J.F., Hosner P.A., Tsai W.L.E., McCormack J.E., Braun E.L., Kimball R.T., Brumfield
1269 R.T., Faircloth B.C. 2022. Historical specimens and the limits of subspecies phylogenomics
1270 in the New World quails (Odontophoridae). Mol. Phylogenet. Evol. 175:107559.

Salter J.F., Oliveros C.H., Hosner P.A., Manthey J., Robbins M.B., Moyle R.G., Brumfield R.T., Faircloth B.C. 2019. Extensive paraphyly in the typical owl family (Strigidae). Auk. 137:ukz070.

Scornavacca C., Galtier N. 2017. Incomplete Lineage Sorting in Mammalian Phylogenomics. Syst. Biol. 66:112–120.

Seppey M., Manni M., Zdobnov E.M. 2019. BUSCO: Assessing Genome Assembly and Annotation Completeness. Methods Mol. Biol. 1962:227–245.

Shakya S.B., Alexander A., Lim H.C., Manthey J.D., Prawiradilaga D., Chan K.O., Sheldon F.H., Moyle R.G. 2023. Demographic history of a complex polymorphism in populations of the Oriental Dwarf Kingfisher (Ceyx erithaca/rufidorsa) of Southeast Asia. Ibis . 165:1267–1279.

Simão F.A., Waterhouse R.M., Ioannidis P., Kriventseva E.V., Zdobnov E.M. 2015. BUSCO: assessing genome assembly and annotation completeness with single-copy orthologs. Bioinformatics. 31:3210–3212.

Simões M., Breitkreuz L., Alvarado M., Baca S., Cooper J.C., Heins L., Herzog K., Lieberman B.S. 2016. The Evolving Theory of Evolutionary Radiations. Trends Ecol. Evol. 31:27–34.

Sin Y.C.K., Eaton J.A., Hutchinson R.O., Rheindt F.E. 2022. Re-assessing species limits in a morphologically cryptic Australasian kingfisher lineage (Coraciiformes: Halcyonidae) using bioacoustic data. Biol. J. Linn. Soc. Lond. 136:489–505.

Smith B.T., Mauck W.M., Benz B.W., Andersen M.J. 2020. Uneven Missing Data Skew Phylogenomic Relationships within the Lories and Lorikeets. Genome Biol. Evol. 12:1131–1147.

Solís-Lemus C., Ané C. 2016. Inferring Phylogenetic Networks with Maximum

1294 Pseudolikelihood under Incomplete Lineage Sorting. PLoS Genet. 12:e1005896.
1295 Solís-Lemus C., Bastide P., Ané C. 2017. PhyloNetworks: A Package for Phylogenetic
1296 Networks. Mol. Biol. Evol. 34:3292–3298.
1297 Stiller J., Feng S., Chowdhury A.-A., Rivas-González I., Duchêne D.A., Fang Q., Deng Y.,
1298 Kozlov A., Stamatakis A., Claramunt S., Nguyen J.M.T., Ho S.Y.W., Faircloth B.C., Haag
1299 J., Houde P., Cracraft J., Balaban M., Mai U., Chen G., Gao R., Zhou C., Xie Y., Huang Z.,
1300 Cao Z., Yan Z., Ogilvie H.A., Nakhleh L., Lindow B., Morel B., Fjeldså J., Hosner P.A., da
1301 Fonseca R.R., Petersen B., Tobias J.A., Székely T., Kennedy J.D., Reeve A.H., Liker A.,
1302 Stervander M., Antunes A., Tietze D.T., Bertelsen M., Lei F., Rahbek C., Graves G.R.,
1303 Schierup M.H., Warnow T., Braun E.L., Gilbert M.T.P., Jarvis E.D., Mirarab S., Zhang G.
1304 2024. Complexity of avian evolution revealed by family-level genomes. Nature.
1305 Suh A., Smeds L., Ellegren H. 2015. The Dynamics of Incomplete Lineage Sorting across the
1306 Ancient Adaptive Radiation of Neoavian Birds. PLoS Biol. 13:e1002224.
1307 Swofford D.L. 2003. {PAUP*. Phylogenetic analysis using parsimony (* and other methods).
1308 Version 4.}. .
1309 Tange O. 2021. GNU Parallel 20210922 ("Vindelev"). Zenodo. .
1310 Taylor S.A., Larson E.L. 2019. Insights from genomes into the evolutionary importance and
1311 prevalence of hybridization in nature. Nat Ecol Evol. 3:170–177.
1312 Thibault J.-C., Cibois A. 2017. Birds of Eastern Polynesia: A biogeographic atlas. Lynx
1313 Edicions.
1314 Timilsena P.R., Wafula E.K., Barrett C.F., Ayyampalayam S., McNeal J.R., Rentsch J.D.,
1315 McKain M.R., Heyduk K., Harkess A., Villegente M., Conran J.G., Illing N., Fogliani B.,
1316 Ané C., Pires J.C., Davis J.I., Zomlefer W.B., Stevenson D.W., Graham S.W., Givnish T.J.,

Leebens-Mack J., dePamphilis C.W. 2022. Phylogenomic resolution of order- and family-level monocot relationships using 602 single-copy nuclear genes and 1375 BUSCO genes. Front. Plant Sci. 13:876779.

Tsai W.L.E., Schedl M.E., Maley J.M., McCormack J.E. 2019. More than skin and bones: comparing extraction methods and alternative sources of DNA from avian museum specimens. Mol. Ecol. Resour.

Van Damme K., Cornetti L., Fields P.D., Ebert D. 2022. Whole-Genome Phylogenetic Reconstruction as a Powerful Tool to Reveal Homoplasy and Ancient Rapid Radiation in Waterflea Evolution. Syst. Biol. 71:777–787.

Van der Auwera G.A., O'Connor B.D. 2020. Genomics in the Cloud: Using Docker, GATK, and WDL in Terra. "O'Reilly Media, Inc."

Walden N., Schranz M.E. 2023. Synteny Identifies Reliable Orthologs for Phylogenomics and Comparative Genomics of the Brassicaceae. Genome Biol. Evol. 15.

Wallace A.R. 1863. On the Physical Geography of the Malay Archipelago. The Journal of the Royal Geographical Society of London. 33:217–234.

Wallace A.R. 1881. Island Life. Harper & Brothers.

Wascher M., Kubatko L. 2021. Consistency of SVDQuartets and Maximum Likelihood for Coalescent-Based Species Tree Estimation. Syst. Biol. 70:33–48.

Waterhouse R.M., Seppey M., Simão F.A., Manni M., Ioannidis P., Klioutchnikov G., Kriventseva E.V., Zdobnov E.M. 2018. BUSCO Applications from Quality Assessments to Gene Prediction and Phylogenomics. Mol. Biol. Evol. 35:543–548.

Whitfield J.B., Lockhart P.J. 2007. Deciphering ancient rapid radiations. Trends Ecol. Evol. 22:258–265.

Whittaker R.J., Fernández-Palacios J.M., Matthews T.J., Borregaard M.K., Triantis K.A. 2017. Island biogeography: Taking the long view of nature's laboratories. Science. 357.

Woodall P.F. 2001. Family Alcedinidae (kingfishers). In: del Hoyo J., Elliott A., Sargatal J., editors. Handbook of the Birds of the World. Vol. 6. Mousebirds to hornbills. Barcelona, Spain: Lynx Edicions. p. 130–249.

Zhang C., Rabiee M., Sayyari E., Mirarab S. 2018. ASTRAL-III: polynomial time species tree reconstruction from partially resolved gene trees. BMC Bioinformatics. 19:153.

Zhao W., Gao J., Hall D., Andersson B.A., Bruxaux J., Tomlinson K.W., Drouzas A.D., Suyama Y., Wang X.-R. 2024. Evolutionary radiation of the Eurasian Pinus species under pervasive gene flow. New Phytol.

Zink R.M., Vázquez-Miranda H. 2019. Species Limits and Phylogenomic Relationships of Darwin's Finches Remain Unresolved: Potential Consequences of a Volatile Ecological Setting. Syst. Biol. 68:347–357.